The Mandatory Role of IL-10–Producing and OX40 Ligand-Expressing Mature Langerhans Cells in Local UVB-Induced Immunosuppression

Ryutaro Yoshiki,* Kenji Kabashima,† Jun-ichi Sakabe,* Kazunari Sugita,* Toshinori Bito,* Motonobu Nakamura,* Bernard Malissen,‡ and Yoshiki Tokura*

The mechanism underlying the local UVB-induced immunosuppression is a central issue to be clarified in photoimmunology. There have been reported a considerable number of cells and factors that participate in the sensitization phase-dependent suppression, including Langerhans cells (LCs), regulatory T cells, IL-10, and TNF-α. The recent important finding that LC-depleted mice rather exhibit enhanced contact hypersensitivity responses urged us to re-evaluate the role of LCs along with dermal dendritic cells (dDCs) in the mechanism of UVB-induced immunosuppression. We studied the surface expression of OX40 ligand (OX40L) and the intracellular expression of IL-10 in LCs and dDCs from UVB-irradiated (300 mJ/cm^2) skin of BALB/c mice and those migrating to the regional lymph nodes from UVB-irradiated, hapten-painted mice. In epidermal and dermal cell suspensions prepared from the UVB-irradiated skin, LCs expressed OX40L as well as CD86 and produced IL-10 at a higher level than Langerin$^-$ dDCs. The UVB-induced immunosuppression was attenuated by the administration of IL-10–neutralizing or OX40L-blocking Abs. In mice whose UVB-irradiated, hapten-painted skin was dissected 1 d after hapten application, the contact hypersensitivity response was restored, because this treatment allowed dDCs but not LCs to migrate to the draining lymph nodes. Moreover, LC-depleted mice by using Langerin-diphtheria toxin receptor–knocked-in mice showed impaired UVB-induced immunosuppression. These results suggest that IL-10–producing and OX40L-expressing LCs in the UVB-exposed skin are mandatory for the induction of Ag-specific regulatory T cells. *The Journal of Immunology*, **2010, 184: 5670–5677.**

Ultraviolet radiation is one of the significant environmental factors affecting humans or other animals. It is well known that UV, in particular the middle wavelength range (290–320 nm, UVB), can be hazardous to human skin by acutely evoking sunburn and epidermal cell death and by chronically inducing skin cancers and skin aging (1–4). UVB radiation also exerts an immunomodulating effect on cutaneous contact hypersensitivity (CHS) by affecting various skin-constituent cells and factors (5). Preirradiation of sensitizing area with low-dose UVB suppresses the development of CHS to hapten in mice (6). In addition to the failure to generate hapten sensitization, mice develop tolerance, because animals treated in this way cannot be resensitized with the same hapten at a later time point. The UVB-induced immunosuppression appears to be hapten-specific, because the sensitization with other nonrelated haptens is not affected (6). Moreover, this hapten-specific immunosuppression can be transferable, as an injection of lymph node cells or splenocytes from UVB-tolerized mice into naive mice inhibits the sensitization with the relevant hapten in the recipients (7). It was once considered that the UVB-induced immunosuppression was mediated by hapten-specific suppressor T cells (5, 8, 9). Now, this suppressor T cell is renamed regulatory T cell (Treg) (10–12). Therefore, a suppressive signal that causes UVB-induced tolerance is hypothesized to exist in the draining lymph node (DLN) of UVB-irradiated skin, where Tregs are induced and suppress the generation or function of effector T cells. However, it remains unclear how the suppressive signal is transmitted from the skin to the DLNs. On one hand, Tregs act in part through the induction of IL-10 production (13). On the other hand, IL-10 is a key cytokine to induce Tregs, and keratinocytes have been considered to be the source of IL-10. However, all the mechanisms underlying UVB-induced immunosuppression are not attributed to keratinocyte-derived IL-10, because human keratinocytes are incapable of producing IL-10 (14). More fundamentally, keratinocytes are unable to migrate to the DLN. Therefore, alternative cells with a migrating ability are likely responsible for mediation of suppressive signals.

Recent studies have revealed the involvement of OX40 (CD134) and its ligand (OX40L) in T cell–APC interaction (15–18). OX40 is expressed on activated CD4$^+$ T cells and on certain populations of CD8$^+$ T cells (15–17, 19), whereas OX40L is expressed on APCs, such as activated B cells (20), dendritic cells (DCs) (21, 22), microglia (23), and endothelial cells (24). Ligation of OX40L on human DCs enhances their maturation and production of cytokines (22), and blockade of OX40L during naive T cell–DC interaction suppresses the development of IL-4–producing T cells (25). It is thus suggested that OX40 and OX40L play an important role in the interaction of DCs with T cells to induce, in particular, Th2 cells. Moreover, CD4$^+$CD25$^+$ Tregs express OX40 at a high level compared with CD4$^+$CD25$^-$ T cells (26, 27). Considering that UVB-induced suppressor T cells were historically identified

*Department of Dermatology, University of Occupational and Environmental Health, Fukuoka; †Department of Dermatology, Kyoto University, Kyoto, Japan; and ‡Centre d'Immunologie de Marseille-Luminy, Institute National de la Santé et de la Recherche Médicale U631, Centre National de la Recherche Scientifique Unité Mixte de Recherche 6102, Université de la Méditerrannée, Marseille Cedex 07, France

Received for publication October 7, 2009. Accepted for publication March 17, 2010.

Address correspondence and reprint requests to Dr. Ryutaro Yoshiki, University of Occupational and Environmental Health, 1-1, Iseigaoka, Yahatanishi-ku, Kitakyushu, Fukuoka 807-8555 Japan. E-mail: yockey@med.uoeh-u.ac.jp

Abbreviations used in this paper: 7-AAD, 7-aminoactinomycin D; CHS, contact hypersensitivity; DC, dendritic cell; dDC, dermal dendritic cell; DLN, draining lymph node; DNFB, dinitrofluorobenzene; DT, diphtheria toxin; DTR, diphtheria toxin receptor; LC, Langerhans cell; OX40L, OX40 ligand; RANKL, RANK ligand; Treg, regulatory T cell.

www.jimmunol.org/cgi/doi/10.4049/jimmunol.0903254

as Th2 cells (28), these findings provide an implication that OX40–OX40L interaction participates in the development of UVB-mediated $CD4^+CD25^+$ Tregs.

Langerhans cells (LCs) are capable of migrating from the epidermis into the DLNs on sensitization (29). Several investigator groups have suggested that LCs are responsible for induction of Tregs (30, 31), but the mechanism underlying the Treg induction by DCs in the UVB-irradiated skin remains unclear in major parts. Recent immunological studies have demonstrated that there are dermal DCs (dDCs), including $Langerin^+$ dDCs and $Langerin^-$ dDCs in the murine skin (32–36). This raises the possibility that not only LCs but also dDCs have an ability to induce Tregs by UVB irradiation of the skin.

In this study, we demonstrate that UVB irradiation of the skin leads to IL-10 production and OX40L expression by LCs. Our study using Langerin-diphtheria toxin receptor (DTR)–knocked-in mice shows that the IL-10–producing and OX40L-expressing LCs play a mandatory role in the induction of Tregs.

Materials and Methods

Animals and reagents

Six- to 10-wk-old BALB/c female mice were purchased from Kyudo (Kumamoto, Japan). Mice were maintained on a 12-h light/dark cycle under specific pathogen-free conditions. Langerin-DTR–knocked-in mice was generated (37). To deplete $Langerin^+$ cells, mice were injected i.p. with diphtheria toxin (DT) (100 ng each; Sigma-Aldrich, St. Louis, MO). Protocols were approved by the Institutional Animal Care and Use Committee of the University of Occupational and Environmental Health, Fukuoka, Japan.

Contact hypersensitivity

Mice were sensitized with dinitrofluorobenzene (DNFB) by applying 50 μl 0.5% DNFB in acetone:olive oil (4:1) to the shaved abdomen on day 0. On day 5, 20 μl 0.2% DNFB was applied to both ears for elicitation. Ear swelling was measured with a micrometer 24 h postelicitation.

UVB irradiation

The shaved abdomen was exposed to UV with a bank of four UVB lamps (Toshiba FL 20S, Toshiba Medical Supply, Tokyo, Japan) (5, 8, 9) that emit most of their energy within the UVB range (290–320 nm), with an emission peak at 313 nm. The irradiance was measured with a UVR-305/365 digital radiometer (Tokyo Kogaku Kikai KK, Tokyo, Japan). Mice were exposed to 300 mJ/cm^2 UV on the shaved abdomen on day −2 presensitization (day 0). Although BALB/c mice are usually not very susceptible to UVB, we found that a single exposure of BALB/c mice to UVB at 300 mJ/cm^2 induces UVB immunosuppression with an elevated percentage of $Foxp3^+$ $CD25^+$ cells in the DLN cells. Because a single irradiation of the skin to UVB and following FITC paining are convenient for the study of DC migration to the DLN, we used this protocol and strain of mice in this study. The ears of mice were protected from radiation with opaque foil.

Culture medium

RPMI 1640 (Life Technologies, Grand Island, NY) was supplemented with 10% heat-inactivated FCS, 2 mM L-glutamine, 5×10^{-5} M 2-ME, 10^{-5} M sodium pyruvate, 25 mM HEPES, 1% nonessential amino acids, 100 U/ml penicillin, and 100 μg/ml streptomycin (all from Life Technologies).

Preparation of whole skin suspensions

Skin sheets from mouse abdomen were floated in 0.2% trypsin in PBS ([pH 7.4]; Sigma-Aldrich) for 30 min at 37°C as described previously (38). The epidermis was separated from the dermis with forceps in PBS supplemented with 10% FCS. Both epidermis and dermis were minced and incubated for 1 h at 37°C in PBS with collagenase II (Sigma-Aldrich). The obtained cells were filtered through a 40-μm filter.

Flow cytometry

Cells were immunostained with various combinations of fluorescence-conjugated mAbs and analyzed with an FACSCanto flow cytometer (BD Biosciences, San Diego, CA) and FlowJo software (Tree Star, Ashland, OR). The expression of cell surface or intracellular molecules and intracytoplasmic cytokines were analyzed using the following Abs: Alexa Fluor 488-conjugated antiepithelial cell adhesion molecule (EpCAM; Biolegend, San Diego, CA); PE-conjugated anti-OX40 ligand (OX40L), anti-CD86, anti-RANK, anti-rat IgG; APC-conjugated anti-MHC class II Ab; biotin-conjugated anti-mouse CD207 (Langerin), anti–IL-10 Ab, and anti-rat IgG; and PE-Cy7–conjugated streptoavidine (eBioscience, San Diego, CA). Intracytoplasmic IL-10 and Langerin was detected in permeabilized cell suspensions using a BD Cytofix/Cytoperm Plus Kit (BD Biosciences).

Cutaneous DC migration into DLNs

Mice were painted on the clipped abdomen with 200 μl 2% FITC (Sigma-Aldrich), and axillar and inguinal lymph nodes were taken 24 h later. Single-cell suspensions were prepared and subjected to flow cytometric analysis.

Apoptosis analysis

Twenty-four hours after UVB irradiation (300 mJ/cm^2), whole skin suspensions were stained with APC-Cy-7–conjugated anti-MHC class II or PE-conjugated EpCAM and FITC-conjugated CD103 (BD Biosciences) for 30 min and stained with Alexa Flour 647-conjugated Annexin V (Invitrogen, Carlsbad, CA) and 7-aminoactinomycin D (7-AAD; BD Biosciences), according to the manufacturer's protocol. Apoptosis in keratinocytes or DCs was analyzed by FACSCanto (BD Biosciences) using FlowJo software (Tree Star) as previously described (39).

In vitro promotion of LC IL-10 production by RANK ligand and its blockade with neutralizing Ab against RANK

Freshly isolated epidermal cell suspensions (5×10^5/well) were cultured with or without 1 μg/ml rRANK ligand (RANKL) (R&D Systems, Minneapolis, MN) for 24 h. For RANK-neutralizing assay, 1 μg/ml anti-RANK Ab or isotype-matched control Ab (R&D Systems) was added to the culture 3 h before the addition of rRANKL. Intracellular IL-10 of LCs was measured by FACS.

In vivo neutralization of IL-10 and blocking of OX40L

Mice received i.p. injections of 25 μg anti-mouse IL-10 Ab (R&D Systems) or 10 μg anti-mouse OX40L Ab (Biolegend) for 4 consecutive days (on days 1–4) after UVB irradiation (on day −2) and DNFB sensitization (on day 0). They were challenged with DNFB on day 5, and the ear swelling responses were measured. For control, mice received the same volume of PBS and were sensitized and challenged with DNFB.

Statistical analysis

All data were statistically analyzed using the Student t test. A p value of <0.05 was considered to be significant. Bar graphs were presented as mean ± SD of the mean value.

Results

$Langerin^+$ dDCs are decreased in number and become apoptotic in UVB-irradiated skin

It is a long-held concept that LCs play a critical role in CHS, as they serve as APCs and migrate to the DLNs (40). However, recent immunological studies have demonstrated that not only LCs but also $Langerin^+$ dDCs and $Langerin^-$ dDCs exist in the skin and may differentially function as APCs. We first investigated the numerical change of LCs, $Langerin^+$ dDCs, and $Langerin^-$ dDCs in UVB-irradiated skin. Whole skin suspensions were prepared from the UVB-irradiated and nonirradiated skin as control 24 h after UVB exposure and analyzed by flow cytometry. Using anti-MHC class II, anti-CD11c, anti-Langerin (CD207), and EpCAM Abs, skin-resident DCs were clearly sorted out of the suspensions (Fig. 1*A*, 1*B*). As assessed by the percentage analysis, the populations of LCs ($Langerin^+$ $EpCAM^+$) and $Langerin^-$ dDCs ($Langerin^-$ $EpCAM^-$) showed no substantial change after UVB irradiation (Fig. 1*C* versus 1*D*), although UVB-irradiated skin-derived DCs had a slightly broader MHC class II expression (Fig. 1*B*). However, the percentage of $Langerin^+$ dDCs was dramatically decreased in UVB-irradiated skin (Fig. 1*C* versus 1*D*). When the absolute number of each LC/DC subset per skin specimen was calculated, UVB irradiation reduced dramatically the number of $Langerin^+$ dDCs and moderately that of LCs and did not affect that of $Langerin^-$ dDCs

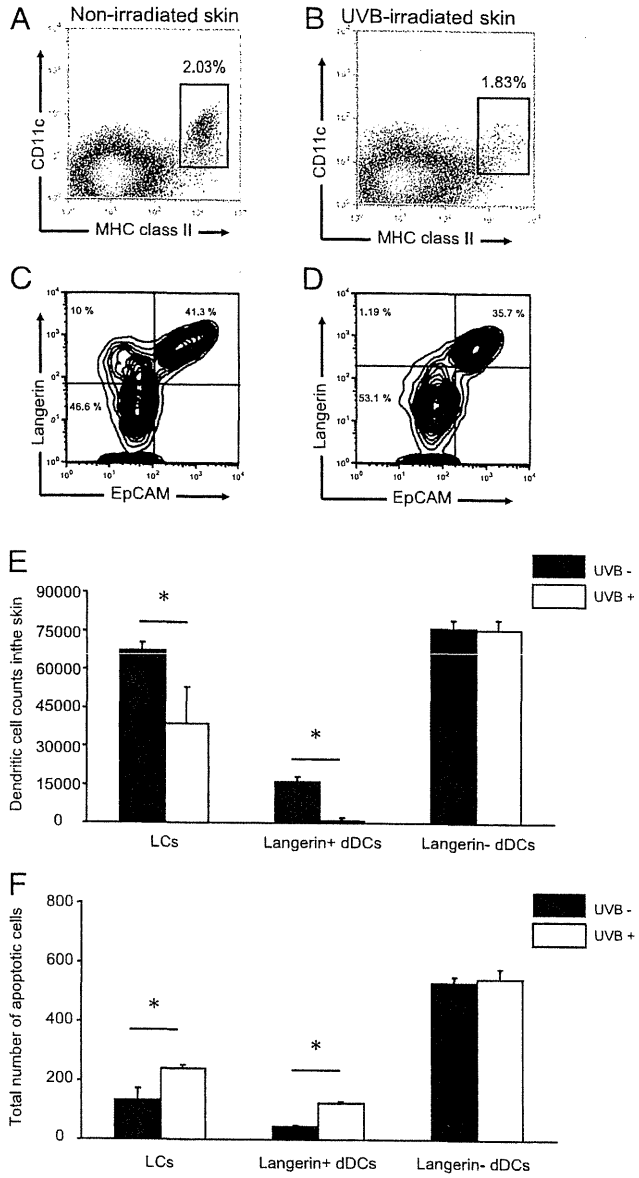

FIGURE 1. Numerical alterations of cutaneous DCs after UVB irradiation of the skin. Single-cell suspensions were stained with APC-conjugated anti-MHC class II and APC-Cy7-conjugated CD11c Abs and subjected to flow cytometric analysis. *A*, Nonirradiated skin. *B*, UVB-irradiated skin. *C*, With the use of anti-EpCAM and anti-Langerin Abs, DCs from nonirradiated skin were clearly sorted out into the three categories: LCs (Langerin$^+$ EpCAM$^+$), Langerin$^+$ dDCs (Langerin$^+$ EpCAM$^-$), and Langerin$^-$ dDCs (Langerin$^-$ EpCAM$^-$). *D*, In UVB-irradiated skin, Langerin$^+$ dDCs were diminished. *E*, Total cell number of each DC subsets. *F*, Apoptotic cell number of LCs and Langerin$^+$ dDCs as assessed by flow cytometric analysis (7-AAD$^-$ and Annexin$^+$). $*p < 0.05$.

(Fig. 1*E*), confirming the decreased number of Langerin$^+$ dDCs in the UVB-irradiated skin. We analyzed apoptosis of LCs and DCs in the UVB-irradiated mice. Six hours after UVB irradiation, we assessed apoptotic cells by flow cytometry and defined them as Annexin V$^+$ and 7-AAD$^-$ cells. Langerin$^+$ dDCs and LCs became apoptotic after UVB irradiation (Fig. 1*F*). There was no selectivity for UVB-induced apoptosis in these two subsets, but when they were compared in the apoptotic cell percentage, Langerin$^+$ DCs were more sensitive to UVB. In contrast to these cells, Langerin$^-$ DCs were resistant to UVB.

LCs but not Langerin$^+$ dDCs migrate from UVB-irradiated skin to DLNs

We examined the numbers and migration timings of LCs, Langerin$^+$ dDCs, and Langerin$^-$ dDCs in the DLNs after FITC application of UVB-irradiated or nonirradiated skin. UVB-irradiated (day −2) and nonirradiated control mice were painted with FITC (day 0). On days 1–4, single-cell suspensions were prepared from the DLNs and stained with anti-CD11c, anti-EpCAM, and anti-Langerin Abs. By flow cytometry, LC subsets (Langerin$^+$ EpCAM$^+$) and Langerin$^+$ dDC subsets (Langerin$^+$ EpCAM$^-$) of CD11c$^+$ FITC$^+$ cells were detected in the DLNs. LCs were gradually increased in number in both UVB-irradiated and nonirradiated groups (Fig. 2*A*). In contrast, the number of Langerin$^+$ dDCs peaked on day 3 in nonirradiated mice, but their number in UVB-irradiated mice was very low (Fig. 2*B*). The number of Langerin$^-$ dDCs in UVB-nonirradiated skin was increased until day 2 and gradually declined, whereas that in UVB-irradiated skin peaked on day 1 and rapidly decreased (Fig. 2*C*). Thus, UVB irradiation allowed LCs and Langerin$^-$ dDCs to migrate into the DLNs, but Langerin$^+$ dDCs in the irradiated skin did not migrate to the DLNs. There was no significant difference in the number of FITC$^-$ DCs of each subset (data not shown). Therefore, the numerical reduction of Langerin$^+$ dDCs in the UVB-irradiated skin did not result from their emigration from the skin. It is assumed that when a hapten is applied to the UVB-preirradiated skin, there are few Langerin$^+$ dDCs capable of migrating to the DLNs and priming Tregs or effector T cells.

UVB upregulates LC maturation and promotes IL-10 production and OX40L expression

It has long been thought that LCs represent one of the most likely targets for UVB in immunosuppression because of their location in the skin and their importance as APCs. Recent studies using LC-depleted mice have shown that LCs are dispensable for CHS (37) and rather downregulate the CHS response (41). In this line of thinking, dDCs may play an essential role for the development of CHS (42). To address the regulatory functions of UVB-irradiated DC populations, we examined the expression of intracellular IL-10 and surface OX40L as well as CD86 in LCs and Langerin$^-$ dDCs.

Epidermal suspensions were prepared from UVB-irradiated and nonirradiated skin and subjected to flow cytometric analysis. Compared to the nonirradiated control skin, LCs from UVB-irradiated skin showed high expression levels of CD86, OX40L, and intracellular IL-10 (Fig. 3*A*). However, such elevations were not observed in Langerin$^-$ dDCs. This suggests that UVB irradiation upregulates the maturation (CD86 expression) of LCs and promotes the production of IL-10 and the expression of OX40L by LCs, but Langerin$^-$ dDCs are not susceptible to UVB.

To examine these IL-10–producing and OX40L-expressing mature LCs in the UVB-irradiated skin retain the ability to migrate to the DLNs and to serve as APCs, FITC, which is not only a hapten but also a cell trafficking marker, was applied to the UVB-irradiated skin 24 h postirradiation. The migrating LCs were identified as the FITC$^+$CD11c$^+$EpCAM$^+$Langerin$^+$ cell fraction, whereas the migrating Langerin$^-$ dDCs were determined as the FITC$^+$CD11c$^+$ EpCAM$^-$Langerin$^-$ cell fraction. The IL-10–producing and OX40L-expressing LCs from UVB-irradiated skin migrated to the DLNs as compared with the nonirradiated skin (Fig. 3*B*), suggesting that LCs of UVB-irradiated skin can induce Treg or Th2 cells in the lymph nodes.

IL-10 production by LCs is mediated by RANKL from UVB-irradiated apoptotic keratinocytes

It has recently been reported that LCs express RANK, and UVB irradiation upregulates cutaneous RANKL, which modulates the

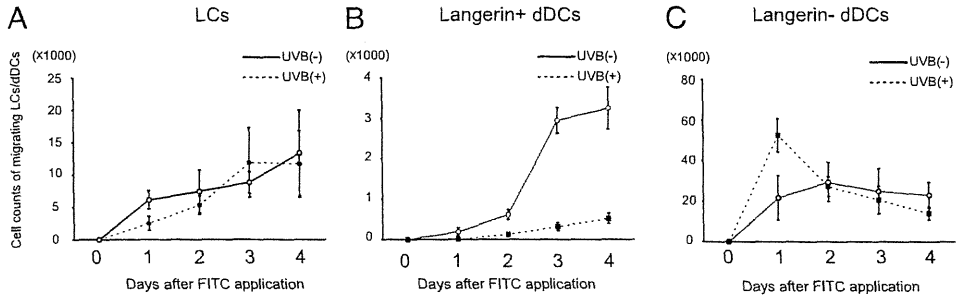

FIGURE 2. Numbers of LCs, Langerin$^+$ dDCs, and Langerin$^-$ dDCs in DLNs after FITC application to UVB-irradiated or nonirradiated skin. Mice were irradiated with UVB (300 mJ/cm^2) on day -2 or nonirradiated and sensitized with FITC on day 0. On days 1–4, DLNs were collected and stained for CD11c, Langerin, and EpCAM. We gated on the FITC$^+$CD11c$^+$ population and counted the EpCAM$^+$ Langerin$^+$ (LCs), EpCAM$^-$ Langerin$^+$ (Langerin$^+$ dDCs), and EpCAM$^-$ Langerin$^-$ (Langerin$^-$ dDCs) cells. *A*, The number of LCs was gradually increased after FITC application in the UVB-irradiated and nonirradiated skin. *B*, The number of Langerin$^+$ dDCs was increased sharply at day 3 in nonirradiated mice but not increased in UVB-irradiated mice. *C*, The number of Langerin$^-$ dDCs peaked at day 1 in the UVB-irradiated mice.

functions of DCs to induce Tregs (43). We have previously reported that when rRANKL was added to LC culture, the RANKL-exposed LCs produce a high amount of IL-10 (44). In contrast, UVB radiation is known to induce apoptosis of epidermal cells. To examine whether epidermal keratinocytes produce RANKL upon UVB exposure in relation to the apoptotic state, epidermal suspensions were prepared from the UVB-irradiated skin 24 h post-exposure and stained to see apoptosis and RANKL expression. By flow cytometry (Fig. 4*A*), keratinocytes were divided into live (Fig. 4*Aa*; 7-AAD$^-$, Annexin$^-$), apoptotic (Fig. 4*Ab*; 7-AAD$^-$, Annexin$^+$), and dead (Fig. 4*Ac*; 7-AAD$^+$, Annexin$^+$) populations. The apoptotic keratinocyte expressed RANKL at a higher degree than did the live and dead keratinocytes (Fig. 4*B*). Thus, UVB-irradiated apoptotic keratinocytes are capable of producing RANKL and subsequently stimulate LCs to produce IL-10 (44). Next, we performed a RANK-blocking study. The production of IL-10 by LCs was promoted by the addition of rRANKL to the culture of epidermal cells, and this increased IL-10 production was blocked by the further addition of an anti-RANK Ab, whereas an isotype-matched control Ab did not suppress IL-10 production (Fig. 4*C*). These results suggest that RANKL from UVB-irradiated keratinocytes mediates IL-10 production by LCs (Fig. 4*C*).

IL-10 neutralization or OX40L blockade abrogates UVB-induced immunosuppression in vivo

It is likely that the production of IL-10 and the expression of OX40L in LCs contribute to the UVB suppression of CHS. To test the significance of IL-10 and OX40L in the suppression, UVB-preirradiated mice (on day -2) were injected i.p. with anti–IL-10 or anti-OX40L Ab for 4 consecutive days (days 0–3), whereas mice were sensitized (day 0) and challenged (day 5) with DNFB. Preirradiation of sensitizing sites to UVB suppressed CHS in mice (Fig. 5). The administration of anti–IL-10 Ab completely restored the CHS response. In contrast, UVB-induced CHS suppression was partially but significantly abrogated by anti-OX40L Ab. We cannot negate the possibility that not only LCs but also other cells are the targets of this blocking procedure, but it seems that IL-10 is profoundly involved in UVB-induced suppression, and OX40L expression is required for the full-blown suppression of CHS.

CHS is successfully induced by dissection of UVB-irradiated and hapten-applied skin at early phase of sensitization

To determine whether LCs and dDCs serve as inducers of Tregs, a skin dissection study was performed for prevention of LC migration at the sensitizing phase. Mice were sensitized with FITC on day 0. When the sensitized skin was dissected on day 1, the total number of migrating LCs was significantly decreased particularly in mice preirradiated with UVB before FITC application (Fig. 6*A*). We therefore examined the CHS response to FITC in mice whose UVB-irradiated and hapten-applied skin was dissected on day 1. This treatment is considered to allow Langerin$^{+/-}$ dDCs to migrate to the DLNs, but most LCs cannot emigrate there. Mice receiving dissection of the sensitizing site did not exhibit UVB-induced immunosuppression of CHS compared with the nondissected and

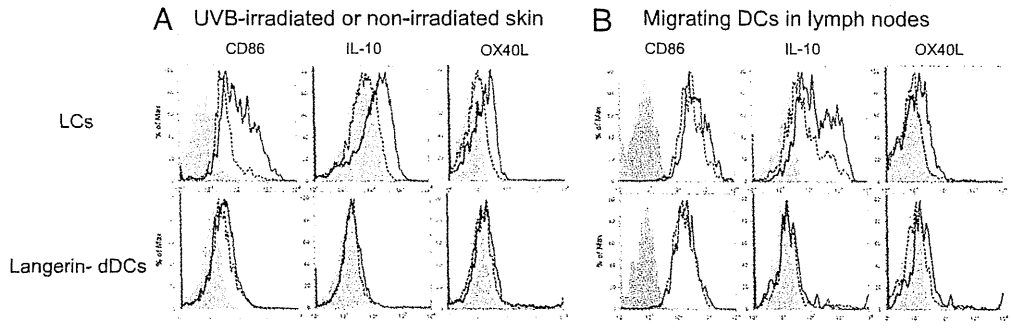

FIGURE 3. Expression of surface CD86, intracellular IL-10, and surface OX40L in LCs and Langerin$^-$ dDCs from the skin and DLNs. *A*, Epidermal cell suspensions were obtained from UVB-irradiated skin 24 h after UVB exposure or nonirradiated skin. Solid line, UVB-irradiated skin; dotted line, non-irradiated skin; and closed shadow, isotype-matched control. *B*, Cell suspensions were obtained from the DLNs of mice receiving UVB irradiation (day -2) and FITC painting (day 0) or mice receiving FITC painting without UVB irradiation. Lymph nodes were taken on day 1, and migrating LCs were identified as FITC$^+$CD11c$^+$EpCAM$^+$Langerin$^+$ cells and migrating Langerin$^-$ dDCs as FITC$^+$CD11c$^+$EpCAM$^-$Langerin$^-$ cells. Solid line, UVB-irradiated mice; dotted line, nonirradiated mice; and closed shadow, isotype-matched control.

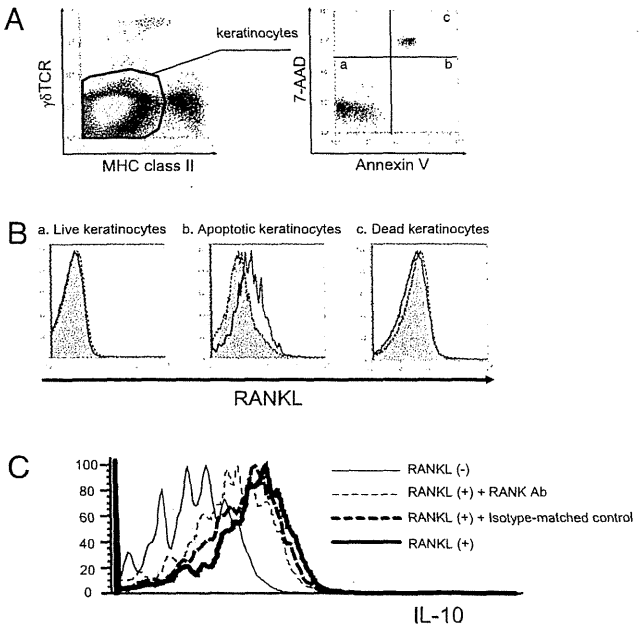

FIGURE 4. RANKL expression in apoptotic keratinocytes from UVB-irradiated skin and RANKL promotion of LC IL-10 production. *A*, Epidermal cell suspensions were obtained from UVB-irradiated (300 mJ/cm^2) skin 24 h postirradiation. Keratinocytes were identified as the MHC class II$^-$ and γδTCR$^-$ fraction by flow cytometry. *a*, Live keratinocyte; *b*, apoptotic keratinocyte, *c*; dead keratinocytes. *B*, Apoptotic keratinocytes expressed RANKL at a higher degree than live and dead keratinocytes. Solid line, UVB-irradiated skin; dotted line, nonirradiated skin; and closed shadow, isotype-matched control. *C*, Epidermal cell suspensions were cultured with or without rRANKL for 24 h. Intracellular IL-10 was measured by FACS. IL-10 production in LC was increased by the addition of rRANKL, and the increased IL-10 production was reduced by the further addition of anti-RANK Ab.

UVB-irradiated mice (Fig. 6*B*). The data suggest that migration of LCs, but not Langerin$^{+/-}$ dDCs, to the lymph nodes is required for UVB-induced CHS suppression.

LC-depleted mice do not exhibit UVB-induced immunosuppression

To discriminate the function of LCs from that of dDCs more clearly, LCs were depleted with DT in Langerin-DTR–knocked-in mice. LCs were completely ablated from the epidermis within 24 h postinjection of DT (Fig. 7*A*, 7*B*). We then addressed the role of LCs in the UVB-induced suppression of CHS. The LC-depleted mice were irradiated with UVB on shaved skin (day −2), painted with DNFB on the same site (day 0), and challenged with DNFB on the ears (day 5). The magnitude of the hapten-specific challenge response was measured 24 h later. As compared with UVB-irradiated non-DT control mice, LC-depleted and UVB-irradiated mice developed a markedly high CHS response (Fig. 7*D*).

We also investigated whether Langerin$^+$ dDCs are involved in the UVB-induced immunosuppression. It has been reported that Langerin$^+$ dDCs recolonize 5 d or less after DT injection (32). Ten days after DT injection, when LCs are still absent in the epidermis but dDC are present (Fig. 7*A* versus 7*C*), mice were preirradiated with UVB and sensitized and elicited with DNFB. Compared to the control mice, LC-depleted but Langerin$^+$ dDC-bearing mice did not show UVB-induced immunosuppression (Fig. 7*E*). Therefore, it is most likely that LCs induce the UVB-induced immunosuppression, but neither Langerin$^+$ nor Langerin$^-$ dDCs have the ability to mediate the suppression.

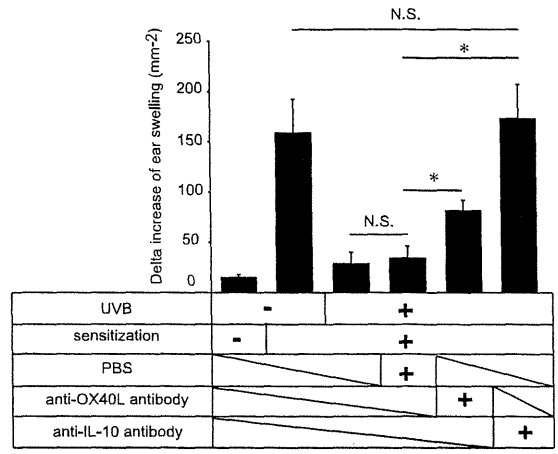

FIGURE 5. Effects of administration of IL-10–neutralizing and OX40L-blocking Abs. Mice were irradiated with UVB (300 mJ/cm^2) on day −2, sensitized with DNFB on day 0, and challenged with DNFB on day 5. IL-10–neutralizing Ab (25 μg per mouse), OX40-blocking Ab (10 μg per mouse), or PBS (for control) was injected i.p. on days 0–3. Positive control mice were sensitized and challenged, and negative control mice were challenged without sensitization. $*p < 0.05$.

Discussion

This study addressed the immunological mechanism underlying the impaired sensitization through UVB-irradiated skin. We found that the UVB-induced immunosuppression of CHS is mediated by IL-10–producing, OX40L-expressing, and CD86 highly expressing mature LCs, which are induced by exposure to RANKL released from UVB-irradiated, apoptotic keratinocytes. The mandatory role of LCs for the UVB-induced suppression was confirmed by the two types of studies, the dissection of sensitizing site and the use of LC-depleted mice. In addition, the recently identified Langerin$^+$ dDCs as well as Langerin$^-$ dDCs (36) seem to play no suppressive role.

Many studies have shown that IL-10 is an essential cytokine in depression of CHS (45–47). The administration of rIL-10 suppresses CHS and induces Ag-specific tolerance (48). IL-10 has also been reported to be a key cytokine in the mechanism of UVB-induced tolerance, as anti–IL-10 Ab treatment before UVB exposure prevents UVB-induced tolerance (49). The neutralizing study using anti–IL-10 Ab further confirmed that IL-10 is essential for the UVB-induced immunosuppression of CHS. Concerning the source of IL-10, a number of studies have demonstrated keratinocytes to be the producer. However, our present study showed that IL-10 is efficiently produced by LCs when the skin is exposed to UVB. The earlier studies on the production of IL-10 by keratinocytes were performed by determining IL-10 mRNA induction and IL-10 protein release in murine keratinocytes shortly postirradiation with UVB (50) or poststimulation with hapten coupling (51). Because cultured keratinocytes were used in those studies, the conclusion may not correctly reflect the in vivo UVB exposure to the skin. In addition, the mechanism of human UVB-induced immunosuppression cannot be explained with the finding obtained from murine keratinocytes. Whereas murine keratinocytes are capable of releasing IL-10 (50, 52), human keratinocytes are an unlikely source of IL-10 following in vivo UVB exposure, as they express little mRNA for IL-10 and secrete no IL-10 protein (14). We have previously reported that IL-10–producing LCs in the grafted skin have a crucial role in the induction of Ag-specific Tregs (44). Together with the present finding, it is suggested that the LCs that migrate from the skin to the DLNs are the important source of IL-10 under the condition of UVB irradiation or skin grafting. Such a finding of

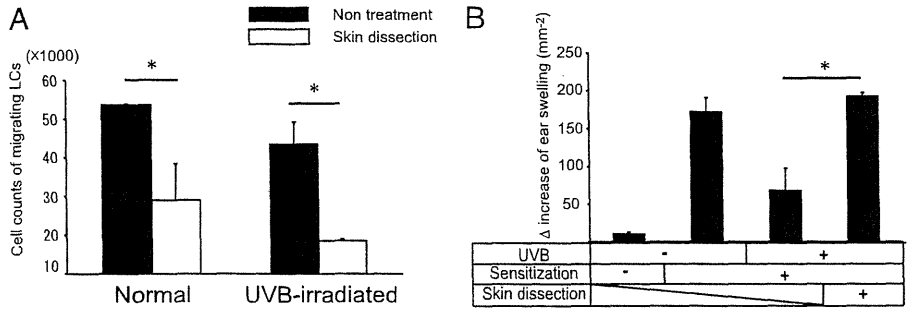

FIGURE 6. Effect of dissection of UVB-irradiated and/or hapten-applied skin on CHS. *A*, The number of LCs migrating to the lymph nodes on day 5 in mice receiving skin dissection on day 1. The LC counts were significantly decreased in mice receiving skin dissection (white bar) compared with non-dissected mice (black bar). *B*, Mice were irradiated with UVB (300 mJ/cm^2) on day −2, sensitized with DNFB on day 0, and challenged with DNFB on day 5. On day 1, a group of mice were skin-dissected. Positive control mice were sensitized and challenged, and negative control mice were challenged without sensitization. $*p < 0.05$.

DC production of IL-10 has also been reported in pulmonary DCs critical for the induction of tolerance (53).

A group of investigators have found that RANKL, which is expressed in keratinocytes of the UVB-irradiated skin, regulates Treg numbers via activation of DCs (43). In another line of studies, i.v. injection of photopheresis-induced apoptotic cells inhibited an immune response to hapten, and this was caused by CD11c$^+$ cells that induce Ag-specific Tregs (54). Likewise, Tregs have been shown to be generated following APC engagement of apoptotic cells (55). Thus, ingestion of apoptotic cells is not merely a scavenging event but also an active process of immune tolerance induction. Teleologically, this process has been described as one of the peripheral tolerance mechanisms (56). We have previously shown that when LCs are exposed to RANKL, they produce IL-10 (44). In this report, we found that apoptotic keratinocytes express RANKL at a higher degree than live keratinocytes and dead keratinocytes. Besides the phagocytosis of apoptotic cells by APCs, RANKL is another tolerogenic signal from apoptotic cells, and the resultant change of DCs to regulatory cells is one of the mechanisms by which apoptosis is related to tolerance.

The blockade of OX40–OX40L interaction by neutralizing OX40 Ab ameliorates experimental allergic encephalomyelitis and experimental colitis, which are Th1-mediated inflammatory diseases (23, 57). OX40 signaling is thus required for the optimal evolution of the Th2 response (58). Moreover, OX40 signaling is involved in the generation of Tregs, and the delivery of OX40 signals can override Treg activity (59). In our data, the blockade of OX40–OX40L interactions partially abrogated the UVB-induced immunosuppression in a comparison with IL-10 neutralization, suggesting that OX40–OX40L interaction is partially responsible for the Treg induction.

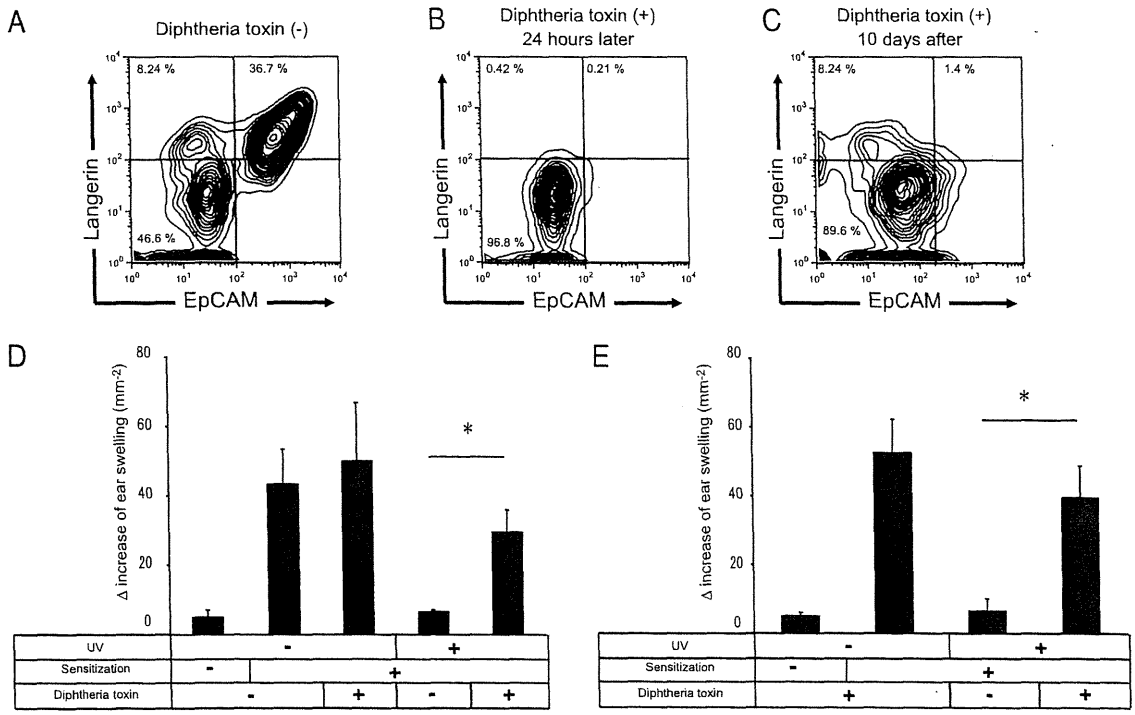

FIGURE 7. UVB-induced immunosuppression in LC-depleted mice. LCs (EpCAM$^+$ Langerin$^+$ cells) and Langerin$^+$ dDCs (EpCAM$^-$ Langerin$^+$ cells) were depleted by DT (100 ng per mouse) in Langerin-DTR–knocked-in mice, Langerin$^+$ dDCs repopulated 10 d later. *A*, Nonirradiated skin. *B*, Twenty-four hours after DT injection. *C*, Ten days after DT injection. *D*, LCs were depleted in Langerin-DTR–knocked-in mice by DT (day −3) before UVB irradiation (day −2). They were sensitized (day 0) and challenged (day 5) with DNFB. *E*, LCs were depleted in Langerin-DTR–knocked-in mice by DT 10 d (day −12) before UVB irradiation (day −2). They were sensitized (day 0) and challenged (day 5) with DNFB. $*p < 0.05$.

We confirmed the crucial role of LCs in the UVB-induced immunosuppression by two strategies. One is that UVB-irradiated, hapten-painted skin was dissected 1 d after hapten application. By this treatment, a considerable number of dDCs could migrate to the DLNs, but LC migration was inhibited, and as a result, the CHS response was restored. In the other study, LCs were more effectively depleted by DT injection to Langerin-DTR–knocked-in mice, and the UVB-induced suppression was markedly abolished in the mice, clearly demonstrating the necessity of LCs for the suppression. Recently, Wang et al. (60) have reported that LCs play no critical role for the UVB-induced immunosuppression. There are major differences in UVB-irradiation doses and mouse strains between their and our studies. Wang et al. (60) irradiated C57BL/6 with UVB at 45 mJ/cm^2 for 3 consecutive days. We irradiated BALB/c mice with UVB at 300 mJ/cm^2 once. Although BALB/c mice are usually not very susceptible to UVB, we found that a single exposure of BALB/c mice to UVB at 300 mJ/cm^2 induces UVB immunosuppression with an elevated percentage of Foxp3$^+$ CD25$^+$ cells in the DLN cells. Because single irradiation of the skin to UVB and following FITC paining is convenient for the study of DC migration to the DLN, we used this protocol and this strain of mice in our study. These differences in the UVB dose and mouse strain possibly give rise to the different results. Alternatively, because their study includes no adoptive transfer experiment, it is unclear whether Tregs are induced in their experimental system. As shown in our study, Langerin$^+$ dDCs become apoptotic after UVB irradiation and cannot migrate to the DLN following hapten application. Given the CHS-inductive role of Langerin$^+$ dermal DCs (37), the abrogation of them by UVB may attenuate the sensitization process of CHS to hapten even without the induction of Tregs. The suppression observed by Wang et al. (60) might be related to this phenomenon. Moreover, the study using the mice deprived of LCs and repopulated with Langerin$^+$ dDCs showed that Langerin$^+$ dDCs are not a requirement for the suppression. Therefore, the UVB immunosuppression in our system is not merely caused by the attenuation of inductive role of Langerin$^+$ dDCs.

The UVB-induced immune tolerance is mediated by Ag-specific Tregs, as the suppression can be adoptively transferred into naive recipients (61). According to the recent observations, UVB-induced Tregs have the CD4$^+$CD25$^+$ phenotype (62), express CTLA-4 (13), and bind to the lectin dectin-2 (61). The Tregs are modulated by IL-10 (46), but also release IL-10 upon antigenic stimulation (13). We have previously reported that cutaneous hypersensitivities to hapten are controlled by Th1 chemokines from keratinocytes and Th2 chemokines from LCs (63). IL-10 released from these LCs at the time of Ag presentation can induce Tregs and also may inhibit the priming of Ag-specific effector T cells. Knowledge of the roles of DCs in immunosuppression may help to further explain the pathways regulating Treg induction and desensitization and provide an insight for immunosuppressive treatments, exemplified by UV therapy for skin diseases.

Disclosures

The authors have no financial conflicts of interest.

References

1. Fisher, G. J., Z. Q. Wang, S. C. Datta, J. Varani, S. Kang, and J. J. Voorhees. 1997. Pathophysiology of premature skin aging induced by ultraviolet light. *N. Engl. J. Med.* 337: 1419–1428.
2. Gilchrest, B. A. 1990. Actinic injury. *Annu. Rev. Med.* 41: 199–210.
3. Kraemer, K. H. 1997. Sunlight and skin cancer: another link revealed. *Proc. Natl. Acad. Sci. USA* 94: 11–14.
4. Kulms, D., and T. Schwarz. 2000. Molecular mechanisms of UV-induced apoptosis. *Photodermatol. Photoimmunol. Photomed.* 16: 195–201.
5. Tokura, Y. 1992. Mechanisms of local, low-dose UVB-induced immunosuppression in contact hypersensitivity. *J. Dermatol.* 19: 923–931.
6. Toews, G. B., P. R. Bergstresser, and J. W. Streilein. 1980. Epidermal Langerhans cell density determines whether contact hypersensitivity or unresponsiveness follows skin painting with DNFB. *J. Immunol.* 124: 445–453.
7. Elmets, C. A., P. R. Bergstresser, R. E. Tigelaar, P. J. Wood, and J. W. Streilein. 1983. Analysis of the mechanism of unresponsiveness produced by haptens painted on skin exposed to low dose ultraviolet radiation. *J. Exp. Med.* 158: 781–794.
8. Satoh, T., Y. Tokura, Y. Satoh, and M. Takigawa. 1990. Ultraviolet-induced suppressor T cells and factor(s) in murine contact photosensitivity. III. Mode of action of T-cell-suppressor factor(s) and interaction with cytokines. *Cell. Immunol.* 131: 120–131.
9. Tokura, Y., Y. Miyachi, M. Takigawa, and M. Yamada. 1987. Ultraviolet-induced suppressor T cells and factor(s) in murine contact photosensitivity. I. Biological and immunochemical characterization of factor(s) extracted from suppressor T cells. *Cell. Immunol.* 110: 305–320.
10. Groux, H., A. O'Garra, M. Bigler, M. Rouleau, S. Antonenko, J. E. de Vries, and M. G. Roncarolo. 1997. A CD4+ T-cell subset inhibits antigen-specific T-cell responses and prevents colitis. *Nature* 389: 737–742.
11. McHugh, R. S., and E. M. Shevach. 2002. The role of suppressor T cells in regulation of immune responses. *J. Allergy Clin. Immunol.* 110: 693–702.
12. Roncarolo, M. G., R. Bacchetta, C. Bordignon, S. Narula, and M. K. Levings. 2001. Type 1 T regulatory cells. *Immunol. Rev.* 182: 68–79.
13. Schwarz, A., S. Beissert, K. Grosse-Heitmeyer, M. Gunzer, J. A. Bluestone, S. Grabbe, and T. Schwarz. 2000. Evidence for functional relevance of CTLA-4 in ultraviolet-radiation-induced tolerance. *J. Immunol.* 165: 1824–1831.
14. Kang, K., C. Hammerberg, L. Meunier, and K. D. Cooper. 1994. CD11b+ macrophages that infiltrate human epidermis after in vivo ultraviolet exposure potently produce IL-10 and represent the major secretory source of epidermal IL-10 protein. *J. Immunol.* 153: 5256–5264.
15. Baum, P. R., R. B. Gayle, III, F. Ramsdell, S. Srinivasan, R. A. Sorensen, M. L. Watson, M. F. Seldin, E. Baker, G. R. Sutherland, K. N. Clifford, et al. 1994. Molecular characterization of murine and human OX40/OX40 ligand systems: identification of a human OX40 ligand as the HTLV-1-regulated protein gp34. *EMBO J.* 13: 3992–4001.
16. Godfrey, W. R., F. F. Fagnoni, M. A. Harara, D. Buck, and E. G. Engleman. 1994. Identification of a human OX-40 ligand, a costimulator of CD4+ T cells with homology to tumor necrosis factor. *J. Exp. Med.* 180: 757–762.
17. Mallett, S., S. Fossum, and A. N. Barclay. 1990. Characterization of the MRC OX40 antigen of activated CD4 positive T lymphocytes—a molecule related to nerve growth factor receptor. *EMBO J.* 9: 1063–1068.
18. Miura, S., K. Ohtani, N. Numata, M. Niki, K. Ohbo, Y. Ina, T. Gojobori, Y. Tanaka, H. Tozawa, M. Nakamura, et al. 1991. Molecular cloning and characterization of a novel glycoprotein, gp34, that is specifically induced by the human T-cell leukemia virus type I transactivator p40tax. *Mol. Cell. Biol.* 11: 1313–1325.
19. Paterson, D. J., W. A. Jefferies, J. R. Green, M. R. Brandon, P. Corthesy, M. Puklavec, and A. F. Williams. 1987. Antigens of activated rat T lymphocytes including a molecule of 50,000 Mr detected only on CD4 positive T blasts. *Mol. Immunol.* 24: 1281–1290.
20. Stüber, E., M. Neurath, D. Calderhead, H. P. Fell, and W. Strober. 1995. Cross-linking of OX40 ligand, a member of the TNF/NGF cytokine family, induces proliferation and differentiation in murine splenic B cells. *Immunity* 2: 507–521.
21. Brocker, T., A. Gulbranson-Judge, S. Flynn, M. Riedinger, C. Raykundalia, and P. Lane. 1999. CD4 T cell traffic control: in vivo evidence that ligation of OX40 on CD4 T cells by OX40-ligand expressed on dendritic cells leads to the accumulation of CD4 T cells in B follicles. *Eur. J. Immunol.* 29: 1610–1616.
22. Ohshima, Y., Y. Tanaka, H. Tozawa, Y. Takahashi, C. Maliszewski, and G. Delespesse. 1997. Expression and function of OX40 ligand on human dendritic cells. *J. Immunol.* 159: 3838–3848.
23. Weinberg, A. D., K. W. Wegmann, C. Funatake, and R. H. Whitham. 1999. Blocking OX-40/OX-40 ligand interaction in vitro and in vivo leads to decreased T cell function and amelioration of experimental allergic encephalomyelitis. *J. Immunol.* 162: 1818–1826.
24. Imura, A., T. Hori, K. Imada, T. Ishikawa, Y. Tanaka, M. Maeda, S. Imamura, and T. Uchiyama. 1996. The human OX40/gp34 system directly mediates adhesion of activated T cells to vascular endothelial cells. *J. Exp. Med.* 183: 2185–2195.
25. Ohshima, Y., L. P. Yang, T. Uchiyama, Y. Tanaka, P. Baum, M. Sergerie, P. Hermann, and G. Delespesse. 1998. OX40 costimulation enhances interleukin-4 (IL-4) expression at priming and promotes the differentiation of naive human CD4(+) T cells into high IL-4-producing effectors. *Blood* 92: 3338–3345.
26. Gavin, M. A., S. R. Clarke, E. Negrou, A. Gallegos, and A. Rudensky. 2002. Homeostasis and anergy of CD4(+)CD25(+) suppressor T cells in vivo. *Nat. Immunol.* 3: 33–41.
27. McHugh, R. S., M. J. Whitters, C. A. Piccirillo, D. A. Young, E. M. Shevach, M. Collins, and M. C. Byrne. 2002. CD4(+)CD25(+) immunoregulatory T cells: gene expression analysis reveals a functional role for the glucocorticoid-induced TNF receptor. *Immunity* 16: 311–323.
28. Yagi, H., Y. Tokura, H. Wakita, F. Furukawa, and M. Takigawa. 1996. TCRV beta 7+ Th2 cells mediate UVB-induced suppression of murine contact photosensitivity by releasing IL-10. *J. Immunol.* 156: 1824–1831.
29. Kabashima, K., T. Murata, H. Tanaka, T. Matsuoka, D. Sakata, N. Yoshida, K. Katagiri, T. Kinashi, T. Tanaka, M. Miyasaka, et al. 2003. Thromboxane A2 modulates interaction of dendritic cells and T cells and regulates acquired immunity. *Nat. Immunol.* 4: 694–701.
30. Probst, H. C., K. McCoy, T. Okazaki, T. Honjo, and M. van den Broek. 2005. Resting dendritic cells induce peripheral CD8+ T cell tolerance through PD-1 and CTLA-4. *Nat. Immunol.* 6: 280–286.

31. Shevach, E. M. 2002. CD4+ CD25+ suppressor T cells: more questions than answers. *Nat. Rev. Immunol.* 2: 389–400.
32. Ginhoux, F., M. P. Collin, M. Bogunovic, M. Abel, M. Leboeuf, J. Helft, J. Ochando, A. Kissenpfennig, B. Malissen, M. Grisotto, et al. 2007. Blood-derived dermal langerin+ dendritic cells survey the skin in the steady state. *J. Exp. Med.* 204: 3133–3146.
33. Kaplan, D. H., A. Kissenpfennig, and B. E. Clausen. 2008. Insights into Langerhans cell function from Langerhans cell ablation models. *Eur. J. Immunol.* 38: 2369–2376.
34. Nagao, K., F. Ginhoux, W. W. Leitner, S. Motegi, C. L. Bennett, B. E. Clausen, M. Merad, and M. C. Udey. 2009. Murine epidermal Langerhans cells and langerin-expressing dermal dendritic cells are unrelated and exhibit distinct functions. *Proc. Natl. Acad. Sci. USA* 106: 3312–3317.
35. Poulin, L. F., S. Henri, B. de Bovis, E. Devilard, A. Kissenpfennig, and B. Malissen. 2007. The dermis contains langerin+ dendritic cells that develop and function independently of epidermal Langerhans cells. *J. Exp. Med.* 204: 3119–3131.
36. Wang, L., L. S. Bursch, A. Kissenpfennig, B. Malissen, S. C. Jameson, and K. A. Hogquist. 2008. Langerin expressing cells promote skin immune responses under defined conditions. *J. Immunol.* 180: 4722–4727.
37. Kissenpfennig, A., S. Henri, B. Dubois, C. Laplace-Builhé, P. Perrin, N. Romani, C. H. Tripp, P. Douillard, L. Leserman, D. Kaiserlian, et al. 2005. Dynamics and function of Langerhans cells in vivo: dermal dendritic cells colonize lymph node areas distinct from slower migrating Langerhans cells. *Immunity* 22: 643–654.
38. Tokura, Y., H. Yagi, H. Hashizume, J. Yagi, F. Furukawa, and M. Takigawa. 1994. Accessory cell ability of Langerhans cells for superantigen is resistant to ultraviolet-B light. *Photochem. Photobiol.* 60: 147–153.
39. Goldszmid, R. S., J. Idoyaga, A. I. Bravo, R. Steinman, J. Mordoh, and R. Wainstok. 2003. Dendritic cells charged with apoptotic tumor cells induce long-lived protective CD4+ and CD8+ T cell immunity against B16 melanoma. *J. Immunol.* 171: 5940–5947.
40. Romani, N., S. Holzmann, C. H. Tripp, F. Koch, and P. Stoitzner. 2003. Langerhans cells - dendritic cells of the epidermis. *APMIS* 111: 725–740.
41. Kaplan, D. H., M. C. Jenison, S. Saeland, W. D. Shlomchik, and M. J. Shlomchik. 2005. Epidermal langerhans cell-deficient mice develop enhanced contact hypersensitivity. *Immunity* 23: 611–620.
42. Fukunaga, A., N. M. Khaskhely, C. S. Sreevidya, S. N. Byrne, and S. E. Ullrich. 2008. Dermal dendritic cells, and not Langerhans cells, play an essential role in inducing an immune response. *J. Immunol.* 180: 3057–3064.
43. Loser, K., A. Mehling, S. Loeser, J. Apelt, A. Kuhn, S. Grabbe, T. Schwarz, J. M. Penninger, and S. Beissert. 2006. Epidermal RANKL controls regulatory T-cell numbers via activation of dendritic cells. *Nat. Med.* 12: 1372–1379.
44. Yoshiki, R., K. Kabashima, K. Sugita, K. Atarashi, T. Shimauchi, and Y. Tokura. 2009. IL-10-producing Langerhans cells and regulatory T cells are responsible for depressed contact hypersensitivity in grafted skin. *J. Invest. Dermatol.* 129: 705–713.
45. Annacker, O., R. Pimenta-Araujo, O. Burlen-Defranoux, T. C. Barbosa, A. Cumano, and A. Bandeira. 2001. CD25+ CD4+ T cells regulate the expansion of peripheral CD4 T cells through the production of IL-10. *J. Immunol.* 166: 3008–3018.
46. Ghoreishi, M., and J. P. Dutz. 2006. Tolerance induction by transcutaneous immunization through ultraviolet-irradiated skin is transferable through CD4+ CD25+ T regulatory cells and is dependent on host-derived IL-10. *J. Immunol.* 176: 2635–2644.
47. Girolomoni, G., P. Gisondi, C. Ottaviani, and A. Cavani. 2004. Immunoregulation of allergic contact dermatitis. *J. Dermatol.* 31: 264–270.
48. Enk, A. H., J. Saloga, D. Becker, M. Mohamadzadeh, and J. Knop. 1994. Induction of hapten-specific tolerance by interleukin 10 in vivo. *J. Exp. Med.* 179: 1397–1402.
49. Niizeki, H., and J. W. Streilein. 1997. Hapten-specific tolerance induced by acute, low-dose ultraviolet B radiation of skin is mediated via interleukin-10. *J. Invest. Dermatol.* 109: 25–30.
50. Rivas, J. M., and S. E. Ullrich. 1992. Systemic suppression of delayed-type hypersensitivity by supernatants from UV-irradiated keratinocytes. An essential role for keratinocyte-derived IL-10. *J. Immunol.* 149: 3865–3871.
51. Enk, A. H., and S. I. Katz. 1992. Identification and induction of keratinocyte-derived IL-10. *J. Immunol.* 149: 92–95.
52. Ullrich, S. E. 1994. Mechanism involved in the systemic suppression of antigen-presenting cell function by UV irradiation. Keratinocyte-derived IL-10 modulates antigen-presenting cell function of splenic adherent cells. *J. Immunol.* 152: 3410–3416.
53. Akbari, O., R. H. DeKruyff, and D. T. Umetsu. 2001. Pulmonary dendritic cells producing IL-10 mediate tolerance induced by respiratory exposure to antigen. *Nat. Immunol.* 2: 725–731.
54. Maeda, A., A. Schwarz, K. Kernebeck, N. Gross, Y. Aragane, D. Peritt, and T. Schwarz. 2005. Intravenous infusion of syngeneic apoptotic cells by photopheresis induces antigen-specific regulatory T cells. *J. Immunol.* 174: 5968–5976.
55. Savill, J., I. Dransfield, C. Gregory, and C. Haslett. 2002. A blast from the past: clearance of apoptotic cells regulates immune responses. *Nat. Rev. Immunol.* 2: 965–975.
56. Steinman, R. M., D. Hawiger, K. Liu, L. Bonifaz, D. Bonnyay, K. Mahnke, T. Iyoda, J. Ravetch, M. Dhodapkar, K. Inaba, and M. Nussenzweig. 2003. Dendritic cell function in vivo during the steady state: a role in peripheral tolerance. *Ann. N. Y. Acad. Sci.* 987: 15–25.
57. Higgins, L. M., S. A. McDonald, N. Whittle, N. Crockett, J. G. Shields, and T. T. MacDonald. 1999. Regulation of T cell activation in vitro and in vivo by targeting the OX40-OX40 ligand interaction: amelioration of ongoing inflammatory bowel disease with an OX40-IgG fusion protein, but not with an OX40 ligand-IgG fusion protein. *J. Immunol.* 162: 486–493.
58. MacPhee, I. A., H. Yagita, and D. B. Oliveira. 2006. Blockade of OX40-ligand after initial triggering of the T helper 2 response inhibits mercuric chloride-induced autoimmunity. *Immunology* 117: 402–408.
59. Takeda, I., S. Ine, N. Killeen, L. C. Ndhlovu, K. Murata, S. Satomi, K. Sugamura, and N. Ishii. 2004. Distinct roles for the OX40-OX40 ligand interaction in regulatory and nonregulatory T cells. *J. Immunol.* 172: 3580–3589.
60. Wang, L., S. C. Jameson, and K. A. Hogquist. 2009. Epidermal Langerhans cells are not required for UV-induced immunosuppression. *J. Immunol.* 183: 5548–5553.
61. Aragane, Y., A. Maeda, A. Schwarz, T. Tezuka, K. Ariizumi, and T. Schwarz. 2003. Involvement of dectin-2 in ultraviolet radiation-induced tolerance. *J. Immunol.* 171: 3801–3807.
62. Schwarz, A., A. Maeda, M. K. Wild, K. Kernebeck, N. Gross, Y. Aragane, S. Beissert, D. Vestweber, and T. Schwarz. 2004. Ultraviolet radiation-induced regulatory T cells not only inhibit the induction but can suppress the effector phase of contact hypersensitivity. *J. Immunol.* 172: 1036–1043.
63. Mori, T., K. Kabashima, R. Yoshiki, K. Sugita, N. Shiraishi, A. Onoue, E. Kuroda, M. Kobayashi, U. Yamashita, and Y. Tokura. 2008. Cutaneous hypersensitivities to hapten are controlled by IFN-gamma-upregulated keratinocyte Th1 chemokines and IFN-gamma-downregulated langerhans cell Th2 chemokines. *J. Invest. Dermatol.* 128: 1719–1727.

Journal: JID Despatch Date: 22/6/2010 CE: XXX Graphic: XXX
Article: npg_jid_jid2010188 Pages: 1–5 Op: ED: XX Q2

Cholinergic Urticaria: Studies on the Muscarinic Cholinergic Receptor M3 in the Anhidrotic and Hypohidrotic Skin

Journal of Investigative Dermatology (2010) **0**, 000–000. doi:10.1038/jid.2010.188

TO THE EDITOR

Cholinergic urticaria (CU) is a sweating-associated, syringeal orifice-coincident wheal mediated by acetylcholine. CU is occasionally associated with depressed sweating, as reported under the name of anhidrosis (complete lack of sweating) or hypohidrosis (incomplete lack of sweating) (Itakura *et al.*, 2000). There have been reported 29 patients with CU with anhidrosis and/or hypohidrosis (CUAH) (Kay and Maibach, 1969; Itakura *et al.*, 2000; Yoshida *et al.*, 2009). One hypothesis for the relationship between the wheal formation and the depressed sweating is that the patients are hypersensitive to unknown substance(s) in their sweat and develop wheals in response to sweat leaking from the syringeal ducts to the dermis possibly by obstruction of the ducts (Adachi *et al.*, 1994; Kobayashi *et al.*, 2002). In fact, some patients with common CU exhibit wheals to intradermal injection of the patients' own diluted sweat as well as acetylcholine and histologically show sweat duct obstruction (Fukunaga *et al.*, 2005). However, none of the reported patients with CUAH were positive to the intradermally injected autologous sweat, suggesting that "sweat hypersensitivity" is not responsible for CUAH. In addition, if sweat hypersensitivity is the mechanism, the anhidrotic area should be the predilection site for wheal, but such an observation has not been reported.

The study design was approved by the review board of University of Occupational and Environmental Health. Measurements in this study were performed after informed consent had been obtained. The study was conducted according to the Declaration of Helsinki guidelines. To address its mechanism, we investigated four nonsmoker male CUAH patients, aged 23 (case 1), 24 (case 2), 50 (case 3), and 36 years (case 4). The exercise challenge and iodine–starch assessment for sweat induction (Kobayashi *et al.*, 2002) revealed that the skin surfaces of all patients were divided into the anhidrotic and hypohidrotic areas (Figure 1a). The skin with normal sweating was not seen in any patient. As represented by case 1, the applied iodine–starch was discolored by sweat in the hypohidrotic but not anhidrotic area (Figure 1b, left), and following exercise challenge, the patients developed pinpoint wheals in only the hypohidrotic areas (Figure 1b, right). Intradermal injection of acetylcholine yielded wheal with sweating at only the hypohidrotic areas (Figure 1c). The injection of autologous sweat or serum did not produce wheal in either hypohidrotic or anhidrotic area. Histologically, a periglandular lymphocytic infiltrate was observed around eccrine glands in the anhidrotic but not hypohidrotic area of all patients (Figure 1d). There was no occlusion of sweat ducts. By immunohistochemistry, the infiltrating lymphocytes consisted of a mixture of $CD4^+$ and $CD8^+$ T cells (CD4/CD8 ratio, 1.21; Figure 1e).

Skin sections were immunohistochemically stained with anti-cholinergic receptor muscarin 3 (CHRM3) antibody (H-210, 1:50; Santa Cruz Biotechnology), which is the most important CHR for sweating (Schiavone and Brambilla, 1991). Eccrine epithelial cells of a normal subject expressed CHRM3 (Figure 2a, left) as well as the epidermis and hair follicle cells (Kurzen *et al.*, 2004). Although the cells in the hypohidrotic area bore CHRM3 at lower but moderate levels (Figure 2a, middle), no staining was seen in the anhidrotic areas (Figure 2a, right). Digitalized specimens were exported to JPG files by NDP view software (Hamamatsu Photonics, Hamamatsu, Japan), and three different areas of the cytoplasm of eccrine epithelial cells were expressed as "red density" (RD) (Hino *et al.*, 2010). CHRM3 expression was significantly lower in the anhidrotic than hypohidrotic areas (Figure 2b). However, specificity is the major issue in this immunohistochemical study. Therefore, real-time PCR was performed. Total RNA from serial sections was extracted in cases 1, 2, and 4 and reverse transcribed into complementary DNA using the Qiagen RNeasy FFPE Kit (Qiagen, Hilden, Germany) and first-strand cDNA synthesis kit RT-PCR (Roche Diagnostics, Indianapolis, IN). The expression levels of *CHRM3* and control *GAPDH* (*glyceraldehyde-3-phosphate dehydrogenase*) were examined using ×20 Assays-on-Demand Gene Expression Assay Mix (Hs00265216_s1 and Hs00266705_g1, respectively; Applied Biosystems, Foster City, CA). We performed PCR using RNAs without reverse transcriptase step for each sample. As represented in Figure 2d, we did not amplify the *CHRM3* gene from any RNA without reverse transcriptase (lane 1), but reverse transcriptase step yielded PCR products at an expected size 72 bp (lane 2), revealing that positive *CHRM3* PCR results of real-time PCR were not derived from contaminated genomic DNA. The levels of *CHRM3* expression were higher in the hypohidrotic than anhidrotic areas (Figure 2e).

As mast cells produce histamine in response to acetylcholine (Fantozzi

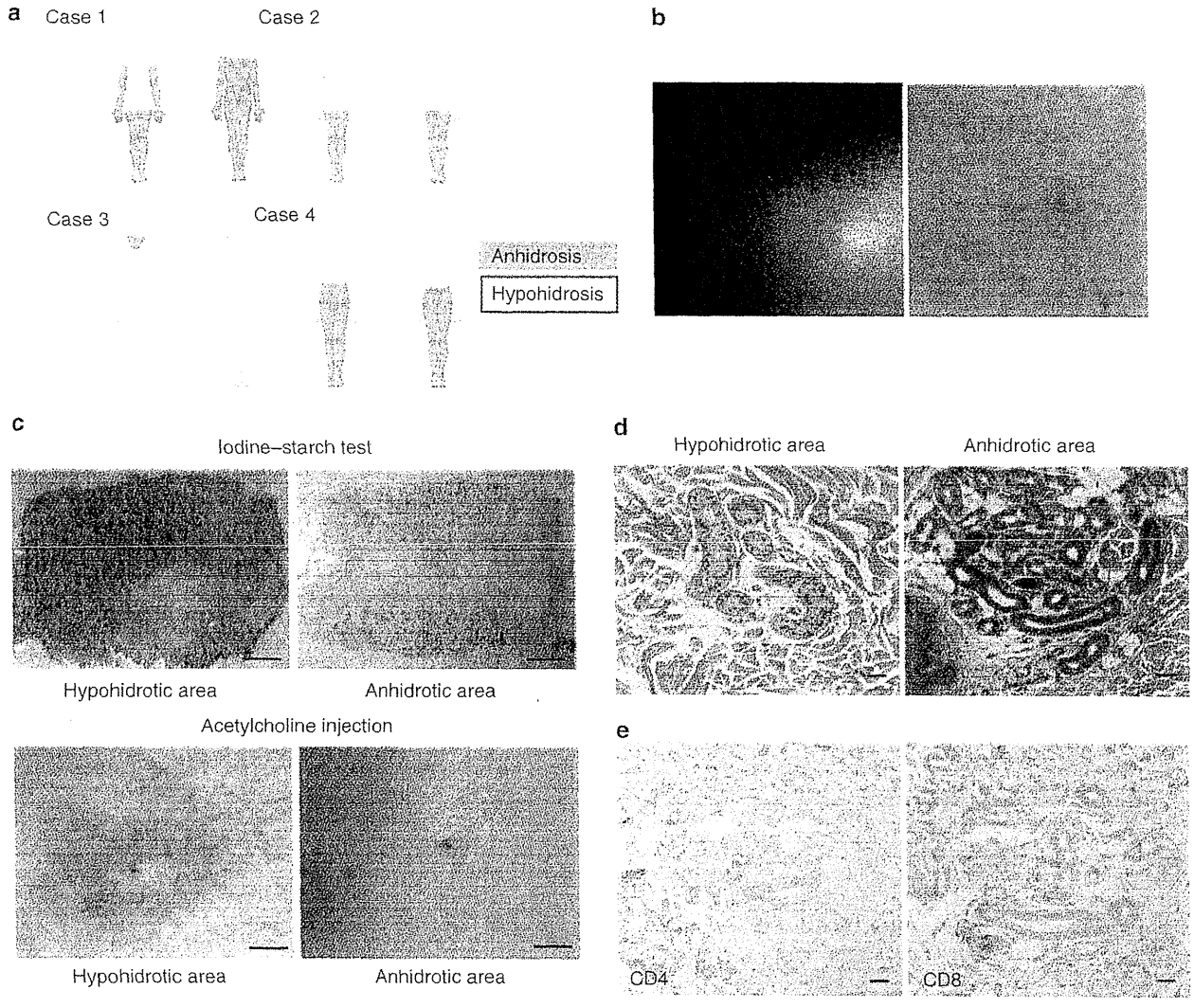

Figure 1. Clinical and histological studies. (**a**) Anhidrotic and hypohidrotic areas in each case. (**b**) Left: Iodine–starch test in case 1. Whereas the applied iodine–starch was discolored by sweat on the left shoulder (hypohidrotic area), such a black color change was not seen on the back, indicating the complete absence of sweating (anhidrotic area). Right: Exercise challenge induced wheals that coincided with sweat orifice on the hypohidrotic area. (**c**) Acethylcholine injection test in the anhidrotic and hypohidrotic areas as represented by case 1. After determination of the anhidrotic and hypohidrotic areas by exercise challenge and iodine–starch application (upper panel), acetylcholine was injected at both sites. Wheal occurred at the hypohidrotic but not anhidrotic area (lower panel). Bar = 1 cm. (**d**) Histological microphotographs of anhidrotic and hypohidrotic areas in case 1. Biopsy specimens were taken from the anhidrotic and hypohidrotic areas (hematoxyline and eosin, original magnification × 100). Note that lymphocytes infiltrate around the sweat glands in the anhidrotic but not hypohidrotic area. Bar = 30 μm. (**e**) Immunophenotype of infiltrating lymphocytes. The infiltrating lymphocytes were immunohistochemically stained for CD4 (left) and CD8 (right). Bar = 30 μm.

et al., 1978; Blandina *et al.*, 1980), we investigated CHR expression in mast cells just in vicinity of eccrine glands. Serial sections were alternatively stained with toluidine blue and with anti-CHRM3 antibody. Mast cells were identified by positive toluidine blue staining (Figure 2c, upper panel), and CHRM3 expression by mast cells was examined in the antibody-stained adjacent sections (Figure 2c, lower panel). In a normal control, mast cells expressed CHRM3 at high levels. Mast cells in conjunction with the secretory portion expressed CHRM3 in the hypohidrotic but not anhidrotic areas. There was no significant difference in the number of mast cells between the anhidrotic and hypohidrotic areas.

Our study revealed that the skin of patients with CUAH is divided into the wheal-non-occuring anhidrotic and wheal-occuring hypohidrotic areas. Even in the hypohidrotic areas, the intradermal injection of autologous sweat did not yield wheal, suggesting the absence of sweat allergy (Tsuchiya *et al.*, 2004). We found the lack of CHRM3 expression in the anhidrotic skin, which may lead to the lack of sensitivity to acetylcholine. Mast cells are responsible for wheal formation and present just in the vicinity of eccrine glands. Neither eccrine gland cells nor mast cells expressed CHRM3 in the anhidrotic area, and it is thus reasonable

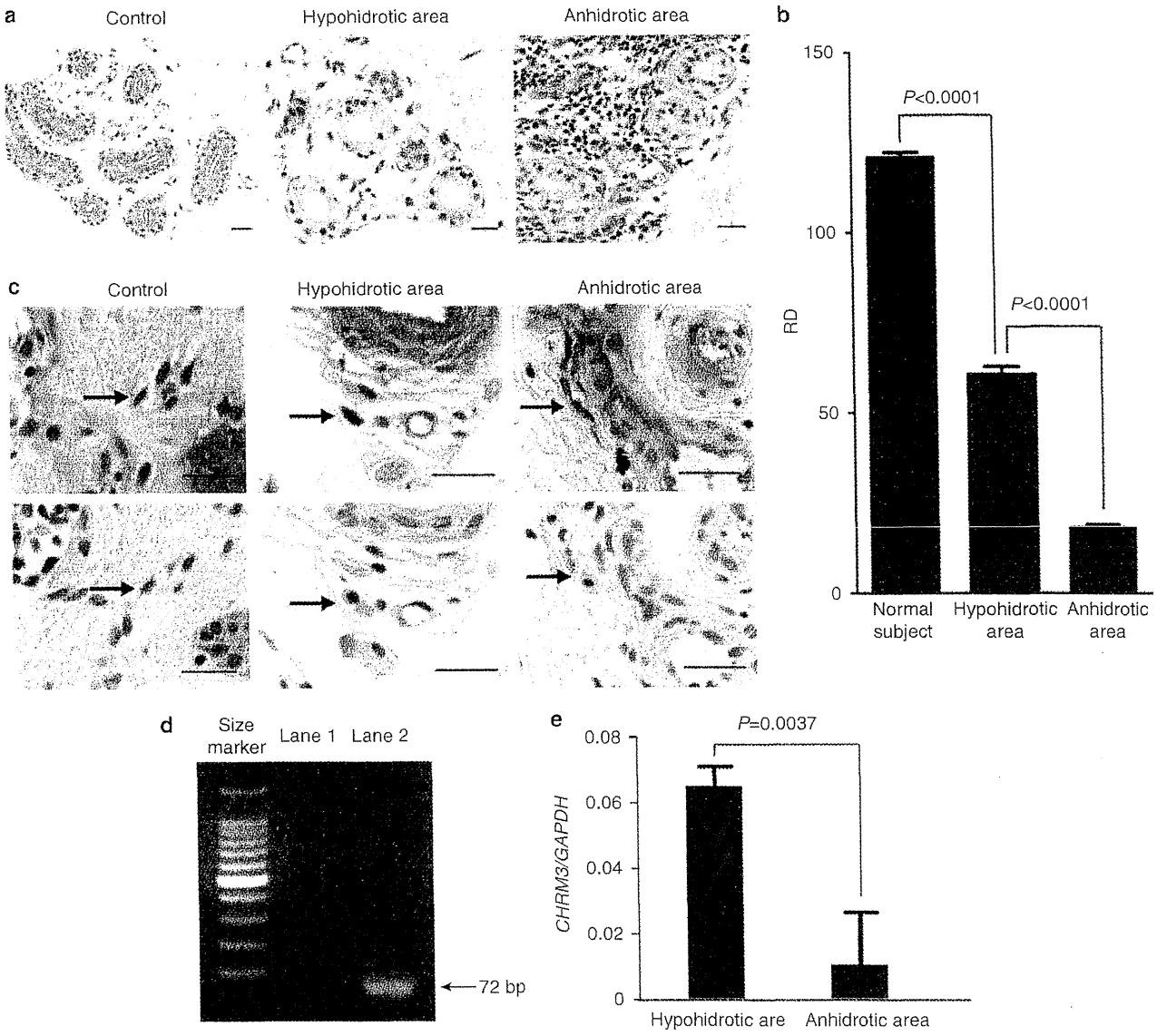

Figure 2. Expression of anti-cholinergic receptor muscarin 3 (CHRM3) in eccrine gland epithelial cells and mast cells. (**a**) CHRM3 expression in eccrine gland epithelial cells. Sections from normal subject's skin (left), and the hypohidrotic skin (middle) and anhidrotic skin (right) of case 1 were immunohistochemically stained with anti-CHRM3 antibody. Bar = 30 μm. (**b**) Staining intensity of CHRM3 expressed as "red density" (RD) in the anhidrotic and hypohidrotic areas of the four cases and in the skin of a normal subject. Three areas of eccrine epithelial cells at the anhidrotic and hypohidrotic areas in each case were subjected to RD analysis, and the mean RD intensity in each case was obtained. Then, the mean ± SD of the four cases was calculated. (**c**) CHRM3 expression in mast cells. Skin sections of a normal subject (control), the hypohidrotic and anhidrotic skin of the patients were stained with toluidine blue (upper panel) or immunohistochemically with CHRM3 (lower panel). Serial sections of each specimen were alternatively stained for CHRM3 and toluidine blue. Mast cells were identified by toluidine blue (arrows). The corresponding sections for toluidine blue and CHRM3 are adjacent. Bar = 30 μm. (**d**) mRNA expression for CHRM3. The end products of real-time PCR using RNA without reverse transcriptase reaction (lane 1) and complementary DNA (cDNA) (lane 2) from hypohidrotic skin of case 1 were electrophoresed in 1.8% agarose gel along with 100 bp DNA ladder (Takara, Kyoto, Japan). *CHRM3* gene products were recognized at an expected size, 72 bp, only in lane 2. (**e**) The expression levels of *CHRM3* and control *GAPDH* (*glyceraldehyde-3-phosphate dehydrogenase*) in the hypohidrotic and anhidrotic areas by real-time PCR analysis. Total RNA from serial sections was extracted in cases 1, 2, and 4 and reverse transcribed into cDNA and first-strand cDNA synthesis kit RT-PCR.

that sweating and wheal formation were absent in this area. CHR mediates wheal development (Tong *et al.*, 1997), and acetylcholine can induce degranulation of mast cells (Fantozzi *et al.*, 1978; Blandina *et al.*, 1980). In the hypohidrotic area, we are tempting to speculate that acetylcholine released from nerves upon exercise cannot be completely trapped by CHR of eccrine glands and overflows to the adjacent mast cells. In this scenario, mast cells may be capable of producing histamine and resultant wheal in response to acetylcholine because of the expression of some degree of CHRM3.

CONFLICT OF INTEREST

The authors state no conflict of interest.

Yu Sawada[1], Motonobu Nakamura[1], Toshinori Bito[1], Shoko Fukamachi[1], Rieko Kabashima[1], Kazunari Sugita[1], Ryosuke Hino[1] and Yoshiki Tokura[1]

[1]Department of Dermatology, University of Occupational and Environmental Health, Kitakyushu, Japan
E-mail: tokura@med.uoeh-u.ac.jp

REFERENCES

Adachi J, Aoki T, Yamatodani A (1994) Demonstration of sweat allergy in cholinergic urticaria. *J Dermatol Sci* 7:142–9

Blandina P, Fantozzi R, Mannaioni PF *et al.* (1980) Characteristics of histamine release evoked by acetylcholine in isolated rat mast cells. *J Physiol* 301:281–93

Fantozzi R, Masini E, Blandina P *et al.* (1978) Release of histamine from rat mast cells by acetylcholine. *Nature* 273:473–4

Fukunaga A, Bito T, Tsuru K *et al.* (2005) Responsiveness to autologous sweat and serum in cholinergic urticaria classifies its clinical subtypes. *J Allergy Clin Immunol* 116:397–402

Hino R, Kabashima K, Kato Y *et al.* (2010) Tumor cell expression of programmed cell death 1 ligand 1 is a prognostic factor for malignant melanoma. *Cancer* 116:1757–66

Itakura E, Urabe K, Yasumoto S *et al.* (2000) Cholinergic urticaria associated with acquired generalized hypohidrosis: report of a case and review of the literature. *Br J Dermatol* 143:1064–6

Kay DM, Maibach HI (1969) Pruritis and acquired anhidrosis; two unusual cases. *Arch Dermatol* 100:291–3

Kobayashi H, Aiba S, Yamagishi T *et al.* (2002) Cholinergic urticaria, a new pathogenic concept: hypohidrosis due to interference with the delivery of sweat to the skin. *Dermatology* 204:173–8

Schiavone A, Brambilla A (1991) Muscarinic M3 receptors mediate secretion from sweat glands in the rat. *Pharmacol Res* 23:233–9

Tong LJ, Balakrishnan G, Kochan JP *et al.* (1997) Assessment of autoimmunity in patients with chronic urticaria. *J Allergy Clin Immunol* 99:461–5

Tsuchiya T, Aoyama K, Hasegawa M *et al.* (2004) Cholinergic urticaria associated with hypohidrosis improved after admission. *Jpn J Clin Dermatol* 58:129–31

Yoshida M, Mizutani K, Watanabe D *et al.* (2009) Cholinergic urticaria associated with Idiopathic generalized anhidrosis. *Practical Dermatol* 31:41–4

ORIGINAL ARTICLE

Inducible Nitric Oxide Synthase Downmodulates Contact Hypersensitivity by Suppressing Dendritic Cell Migration and Survival

Kazunari Sugita[1], Kenji Kabashima[1,4], Ryutaro Yoshiki[1], Atsuko Ikenouchi-Sugita[2], Masato Tsutsui[3], Jun Nakamura[2], Nobuyuki Yanagihara[3] and Yoshiki Tokura[1]

Nitric oxide (NO) has several important roles in various physiological settings; one of the NO synthases, inducible NO synthase (iNOS), is induced by external stimulation of the skin. A prototypic example of external stimulation is hapten exposure, which induces the T-cell-mediated immune response known as contact hypersensitivity (CHS). We herein report on cutaneous dendritic cell (DC) function in the presence of an iNOS-specific inhibitor during the sensitization phase of CHS. First, we examined epidermal cell (EC) suspensions using flow cytometry with an iNOS antibody and confirmed that iNOS was expressed in the cytoplasm of Langerhans cells (LCs). We then studied the role of iNOS in CHS, and found that responses to DNFB were enhanced by the addition of an iNOS inhibitor during sensitization. Similarly, the iNOS inhibitor augmented FITC-induced migration of cutaneous DCs, including Langerin$^+$ LCs and Langerin$^-$ dermal DCs, to draining lymph nodes. Finally, we showed that iNOS inhibitor enhanced LC survival *in vitro*. We concluded that NO suppresses migration and survival of cutaneous DCs, resulting in a downmodulation of CHS.

Journal of Investigative Dermatology (2010) **130,** 464–471; doi:10.1038/jid.2009.288; published online 3 September 2009

INTRODUCTION

Inducible nitric oxide (NO) synthase (iNOS) is one of the three isoenzymes that generate NO from its precursor L-arginine. In the skin, keratinocytes (Arany *et al.*, 1996), Langerhans cells (LCs) (Qureshi *et al.*, 1996), dermal fibroblasts (Wang *et al.*, 1996), and melanocytes (Rocha and Guillo, 2001) express iNOS upon stimulation with inflammatory cytokines and/or lipopolysaccharide (LPS). Although NO can be proinflammatory when produced in large amounts, it may also regulate adaptive immune responses (Kuchel *et al.*, 2003). The best characterized example is the induction of iNOS by LPS and IFN-γ in murine macrophages (Lu *et al.*, 1996), LCs (Qureshi *et al.*, 1996), and keratinocytes (Yamaoka *et al.*, 2000). Although some information has thus been accumulated regarding the *in vitro* effects of iNOS on skin immunocompetent cells, the *in vivo* actions of iNOS remain unknown.

Murine contact hypersensitivity (CHS) is an antigen-specific immune response consisting of the two phases, namely, sensitization and elicitation. The constituents involved in its pathogenesis are Th1/Tc1 cells serving as helper/effector cells (Akiba *et al.*, 2002); cutaneous dendritic cells (DCs), including epidermal LCs and dermal DCs (dDCs), as antigen-presenting cells (Kissenpfennig and Malissen, 2006); and keratinocytes as a source of IL-1α, tumor necrosis factor-α, and GM-CSF to the LCs (Sugita *et al.*, 2007). iNOS is induced in LCs and keratinocytes by contact allergens; this supports the view that iNOS has a role in CHS (Morita *et al.*, 1996). It has previously been reported that an iNOS inhibitor injected intradermally during the elicitation phase suppressed CHS responses (Ross *et al.*, 1998), but the specificity of this iNOS inhibitor is not clear; furthermore, the role of iNOS in the sensitization phase remains unknown.

In this study, we investigated the effects of an iNOS-specific inhibitor in order to determine whether iNOS functions as a positive or negative regulator in CHS. Our results show that iNOS suppresses the CHS response by downmodulating the migration and survival of DCs.

RESULTS

iNOS inhibitor enhances CHS response to DNFB

First, we tested the degree of CHS response in mice treated with L-N^6-iminoethyl-lysine (L-NIL), an iNOS inhibitor.

[1]*Department of Dermatology, University of Occupational and Environmental Health, Kitakyushu, Japan;* [2]*Department of Psychiatry, University of Occupational and Environmental Health, Kitakyushu, Japan;* [3]*Department of Pharmacology, University of Occupational and Environmental Health, Kitakyushu, Japan and* [4]*Department of Dermatology, Kyoto University Graduate School of Medicine, Kyoto, Japan*

Correspondence: Dr K Sugita, Department of Dermatology, University of Occupational and Environmental Health, 1-1 Iseigaoka, Yahatanishi-ku, Kitakyushu 807-8555, Japan. E-mail: k-sugita@med.uoeh-u.ac.jp

Abbreviations: Ab, antibody; B6, C57BL/6; CCL21, CC chemokine ligand 21; CCR7, CC chemokine receptor 7; CHS, contact hypersensitivity; DC, dendritic cell; dDC, dermal DC; EC, epidermal cell; iNOS, inducible nitric oxide synthase; LC, Langerhans cell; L-NIL, L-N^6-iminoethyl-lysine; LPS, lipopolysaccharide; NO, nitric oxide; PBS, phosphate-buffered saline

Received 2 March 2009; revised 9 July 2009; accepted 19 July 2009; published online 3 September 2009

The mice were sensitized and challenged with DNFB, and their ear swelling responses were measured 24 hours after the challenge. A significantly higher degree of ear swelling response was observed in C57BL/6 (B6) mice treated intraperitoneally with L-NIL throughout the sensitization phase than in non-treated control mice (Figure 1a). Similar results were obtained 48 hours after the challenge (data not shown). In addition, histological analysis of the L-NIL-treated mice showed a remarkable infiltration of lymphocytes into the edematous dermis, which was not seen in untreated mice (Figure 1b). To confirm that L-NIL was biologically active in the skin when administered systemically, we measured the NOx ($NO_2^- + NO_3^-$) concentration of DNFB-sensitized skin. NOx production induced by DNFB was inhibited by an intraperitoneal injection of L-NIL (Supplementary Figure S1), suggesting that L-NIL is biologically active in lesional skin even when it is administered systemically.

iNOS expression in keratinocytes and LCs

Freshly isolated murine epidermal cells (ECs) were incubated for 24 hours in a culture medium, and the LCs and keratinocytes among them were analyzed for iNOS expression with flow cytometry. Both the keratinocytes and the LCs bore iNOS in the cytoplasm (Figure 2a). iNOS expression was greater in the mature LCs (major histocompatibility complex (MHC) class II high expression) than in the immature LCs (MHC class II intermediate expression). We carried out the same analysis on ECs that had been cultured for 24 hours in the presence of LPS, and found that LPS increased the number of LCs that highly expressed iNOS (Figure 2b).

iNOS inhibitor increases cutaneous DC accumulation in regional lymph nodes

To investigate the *in vivo* significance of iNOS for cutaneous DCs, we performed an FITC-induced cutaneous

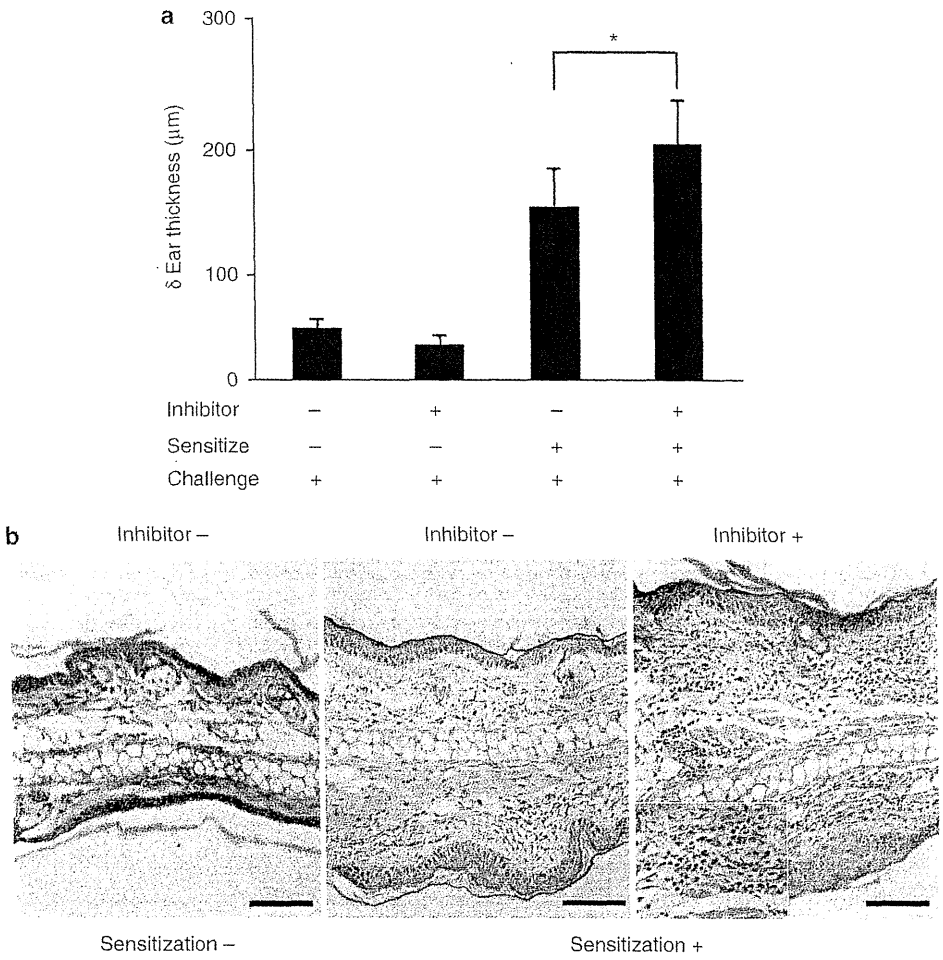

Figure 1. Increased CHS response to DNFB caused by blockade of iNOS. (**a**) For CHS model, B6 mice were immunized by the application of 0.5% DNFB to their shaved abdomens. They were challenged on both ears with 0.3% DNFB. iNOS inhibitor was applied through intraperitoneal injection (2.5 mg in 0.5 ml PBS twice daily). Ear thickness swelling was measured 24 hours later. Data are expressed as the mean ± SD of five mice. $*P<0.05$. (**b**) Non-sensitized ears, challenged ears, and challenged ears from non-treated mice (inhibitor –) were stained with hematoxylin and eosin. Inset: close-up view of hematoxylin and eosin staining of ears from mice treated with iNOS inhibitor, showing perivascular lymphocytic infiltration. Bar = 80 μm. Data are from three independent experiments.

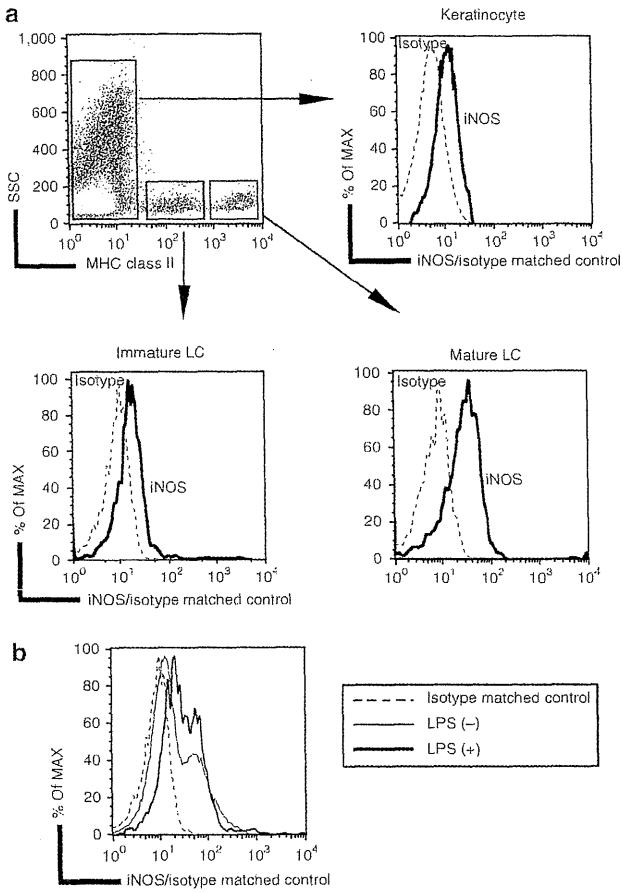

Figure 2. Expression of iNOS by both keratinocytes and LCs. (**a**) EC suspensions were analyzed for the expression of iNOS by means of flow cytometry. For intracellular detection of iNOS, cell fixation–permeabilization was performed before immunolabeling with anti-iNOS and anti-MHC class II mAbs. LCs or keratinocytes were gated by MHC class II positivity. (**b**) EC suspensions from naive mice were cultured with or without LPS (1 $\mu g\,ml^{-1}$) for 24 hours. The cultured cells were subjected to a flow cytometric analysis, which allowed us to measure the expression of iNOS. Data are from three independent experiments.

DC migration assay. FITC applied to the skin is taken up by cutaneous DCs, which subsequently migrate to the draining lymph nodes as $FITC^+$ MHC class II^+ cells. We intraperitoneally injected L-NIL, an iNOS inhibitor (2.5 mg in 0.5 ml phosphate-buffered saline (PBS) twice daily for 4 consecutive days) or the equivalent amount of PBS into mice; 24 hours after the last injection, we applied FITC to the abdomen. We then isolated axillary and inguinal draining lymph node cells 72 hours after FITC application and characterized the $FITC^+$MHC class II^+ cutaneous DCs therein by flow cytometry. Staining for Langerin showed that two subsets of the $FITC^+$ MHC class II^+ cutaneous DCs, the dDCs and LCs, were present in significantly greater numbers because of treatment with iNOS inhibitor (Figure 3a and b). Therefore, the blockade of iNOS promoted lymph node accumulation of cutaneous DCs in response to skin exposure to an antigen.

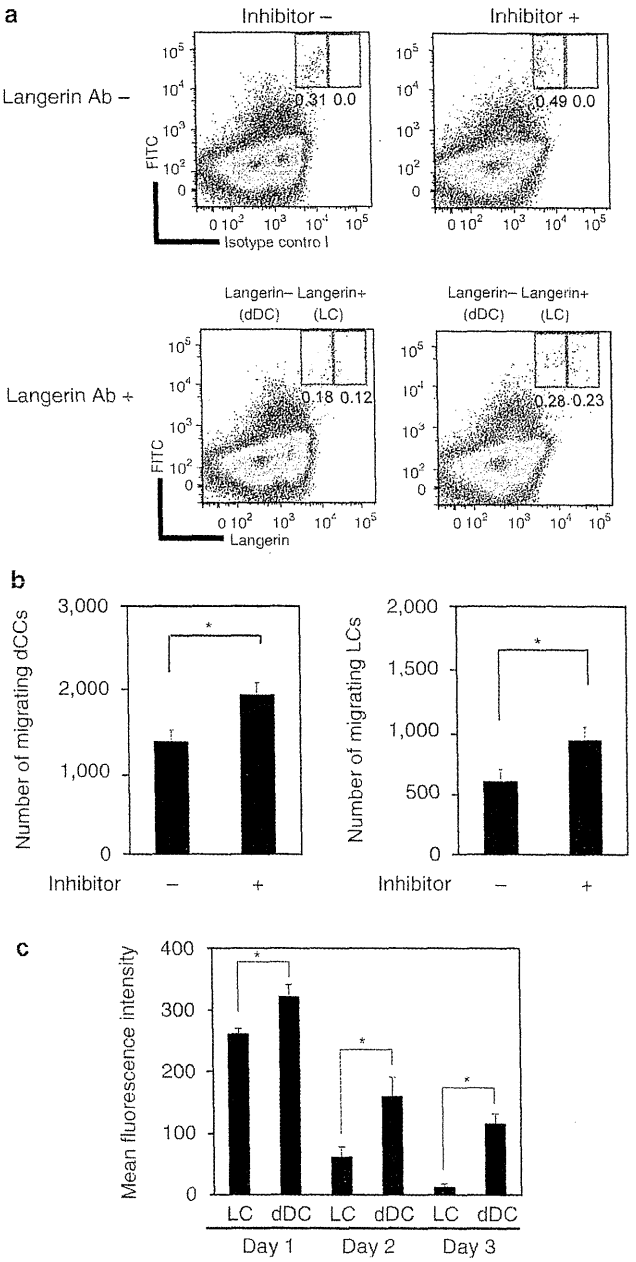

Figure 3. Augmented cutaneous DC accumulation in regional lymph nodes by iNOS blockade. (**a**) Langerin expression and FITC fluorescence in cells derived from regional lymph nodes were analyzed by means of flow cytometry 72 hours after the application of 200 µl of 2% FITC. The percentage of migrating LCs is indicated. (**b**) Migrating dDCs or LCs were counted 72 hours after FITC painting. Columns show the mean ± SD from at least four mice per group. $*P<0.05$. (**c**) Expression of iNOS in migrating LCs and dDCs. Draining lymph node cells were taken from mice painted with FITC on the abdomen and stained with anti-MHC class II, Langerin, and iNOS mAbs. Days 1, 2, and 3 indicate the number of days since FITC painting. Data are expressed as mean fluorescence intensity (MFI) for iNOS. MFI was the value of LCs or dDCs subtracted from that of the isotype-matched control. Columns show the mean ± SD. $*P<0.01$. Results are representative of three independent experiments.

iNOS expression in migrating LCs and dDCs

We examined iNOS expression in freshly isolated LCs and dDCs, both of which are capable of migrating into the lymph nodes on sensitization. The expression of iNOS in these cells was examined with FITC and anti-Langerin mAb. FITC was applied to the abdomen, and draining lymph node cells were sampled 24, 48, and 72 hours later. These cells were then labeled with anti-MHC class II mAb, anti-Langerin Ab, and anti-iNOS Ab. Although LCs are positive for Langerin, most dermal DCs are negative for Langerin (Nagao *et al.*, 2009), iNOS was present in both LCs and dDCs. The mean fluorescence intensity for iNOS was as follows: LC, 11.9 ± 4.1; dDC, 36.6 ± 20.5 (mean ± SD of three mice). These data suggested that iNOS was weakly expressed only in freshly isolated LCs and dDCs, in amounts too small to be statistically significant. Nevertheless, we were able to observe that the dDCs showed a higher mean fluorescence intensity of iNOS expression than the LCs did (Figure 3c).

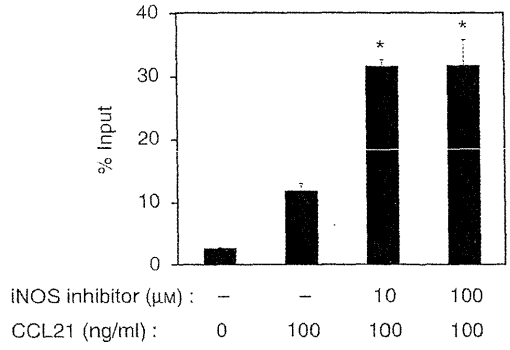

Figure 4. Chemotactic activity of epidermal LCs to CCL21. EC suspensions were incubated with or without iNOS inhibitor plus LPS in culture medium for 9 hours and applied to a transwell. CCL21 at 100 ng ml^{-1} was administered to the lower chamber. Migrating epidermal LCs in the lower chamber were identified as belonging to the MHC class II$^+$ subset. The number of migrating LCs was calculated. Columns represent the mean ± SD of triplicated transwells, and data are from three independent experiments. *$P<0.01$.

Chemotactic activity of LCs to CCL21

EC suspensions were incubated with LPS in a culture medium for 9 hours and applied to transwells in the presence or absence of L-NIL, an iNOS inhibitor. The migrating LCs in the lower chamber were identified as MHC class II$^+$ cells. CCL21 (CC chemokine ligand 21), a cytokine expressed in secondary lymphoid organs that mediates the chemotaxis of lymphocytes and DCs through its receptor, CCR7 (CC chemokine receptor 7; Saeki *et al.*, 1999), was then added to the lower chamber. All LCs exhibited a strong chemotactic response to this chemokine, but this response was significantly increased by the iNOS inhibitor (Figure 4).

iNOS inhibitor caused no alteration of the expression of co-stimulatory molecules or CCR7

The chemotaxis-promoting activity of the iNOS inhibitor, described above, raised the possibility that the iNOS inhibitor upregulates the expression of co-stimulatory molecules and CCR7. To determine whether this is the case, freshly isolated ECs were cultured for 24 hours in the presence or absence of the iNOS inhibitor, and the expression levels of these molecules were monitored by gating for MHC class II$^+$ LCs. After 24 hours of culture, a single population of LCs usually divides into two populations, with different expression levels of co-stimulatory molecules and CCR7 (Sugita *et al.*, 2007) (Figure 5a). The addition of the iNOS inhibitor did not alter the expression of CD86, CD80, CD40, or CCR7 (Figure 5a and b). In chemotaxis, however, the expression of

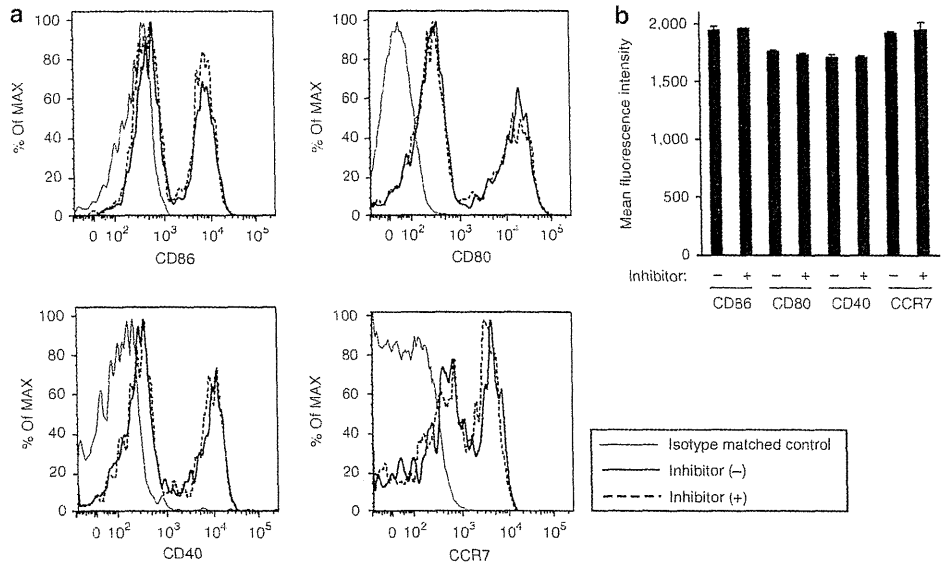

Figure 5. No modulation of CD86, CD80, CD40, or CCR7 expression in LCs by iNOS inhibitor. (a and b) EC suspensions from naive mice were cultured for 24 hours with or without iNOS inhibitor. The cultured LCs were examined for their expression levels of CD86, CD80, CD40, and CCR7. Data are representative of three independent experiments.

CCR7 in DCs is not sufficient to guarantee its functionality (Sanchez-Sanchez *et al.*, 2006); therefore, it is possible that iNOS alters certain downstream functions of LCs without affecting CCR7 expression.

iNOS inhibitor reduces LPS-induced apoptosis of LC

We then evaluated the effect of endogenous iNOS activity on the viability of LCs. EC suspensions from the earlobes of B6 mice were cultured for 9 hours with or without LPS in the presence or absence of L-NIL, an iNOS inhibitor. LPS stimulation reduced the number of LCs, but this reduction was reversed by the addition of the iNOS inhibitor (Figure 6a). It has been reported that epidermal LCs are unable to proliferate *in vitro* when they are incubated as an EC suspension (Schuler and Steinman, 1985), suggesting that the observed effects of the iNOS inhibitor stem from a survival change.

To examine whether the iNOS inhibitor promotes the survival of LCs, cellular viability was assessed through flow cytometry after Annexin V/propidium iodide staining and 9 hours of culture (Figure 6b). This flow cytometry experiment used anti-MHC class II and anti-CD11c mAbs. The percentage of Annexin V and propidium iodide double-positive cells in samples that had been treated with 100 μM iNOS inhibitor and those that had not was as follows: 100 μM, 1.6 ± 0.4%; no addition, 2.2 ± 1.0% (mean ± SD, $n = 3$). These results suggest that the reduction of apoptotic cells that occurs through iNOS inhibitor treatment is not due to the increment of necrotic cells. We found that LPS-induced apoptosis of LCs was reduced by the addition of the iNOS inhibitor (Figure 6c), suggesting that the iNOS inhibitor promotes DC survival.

DISCUSSION

The results of this study on the effects of an iNOS inhibitor include several major findings about the involvement of NO in the sensitization phase of CHS. First, CHS as a model of acquired skin immune response was enhanced by treatment with the iNOS inhibitor. Second, the iNOS inhibitor markedly increased the number of migrating cutaneous DCs. Accordingly, the chemotactic response of LCs to CCL21 was enhanced by *in vitro* incubation with the iNOS inhibitor. Finally, the iNOS inhibitor was capable of reducing LPS-induced apoptosis of LCs.

It has generally been believed that iNOS is involved in CHS as a producer of NO and a trigger of inflammatory responses (Cals-Grierson and Ormerod, 2004). It has been

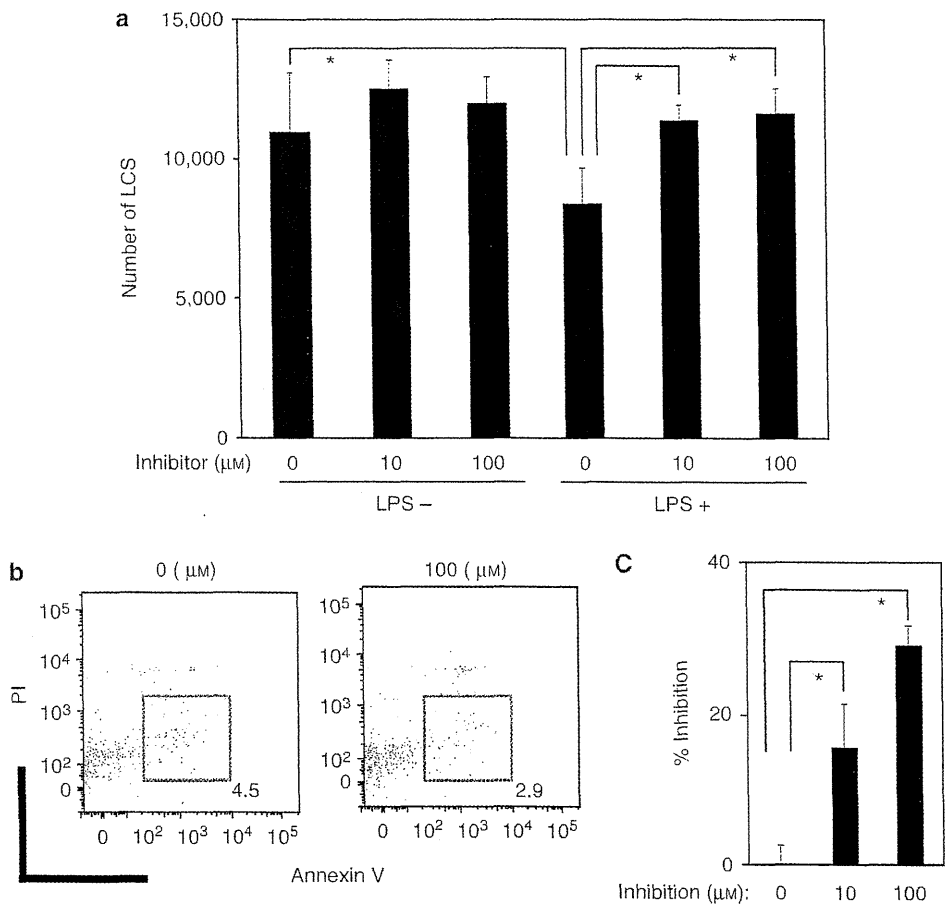

Figure 6. The effect of LPS on LC survival. (a) EC suspensions were cultured with or without LPS and iNOS inhibitor for 9–12 hours. iNOS inhibitor dose dependently increased the number of LCs. Columns show the mean ± SD. *$P<0.05$. Data are representative of three independent experiments. (b) Apoptosis was determined using annexin V/propidium iodide double staining. (c) The percentage inhibition is calculated. Data represent the mean ± SD. *$P<0.05$.

reported that iNOS and NO were produced in human skin subjected to positive patch tests to contact allergens (Cruz *et al.*, 2007; Ormerod *et al.*, 1997) and to the irritant sodium lauryl sulfate; nevertheless, it remains controversial whether iNOS is inhibitory or augmentative in CHS (Ross and Reske-Kunz, 2001). It has also been reported that an iNOS inhibitor exerted a suppressive effect on the CHS response to 2,4,6-trinitrochlorobenzene (TNCB) (Musoh *et al.*, 1998), although this effect was limited to the first few hours of the response, and neither NO production, NO-expressing cells, nor NOS isoenzymes were identified. Thus, the mode of action of iNOS in CHS remains a matter of debate.

It is possible that iNOS first modulates keratinocytes so that they produce cytokines, thereby subsequently modifying LC function. Yet, we found that the production levels of GM-CSF and tumor necrosis factor-α in the culture supernatant of primary keratinocytes of B6 mice cultured for 72 hours were not significantly affected by the presence of the iNOS inhibitor (Supplementary Figure S2). With regard to the effect of iNOS on T cells, we cultured immune $CD4^+$ T cells for 72 hours with varying concentrations of the iNOS inhibitor in the presence of anti-CD3 mAb and found that the iNOS inhibitor was incapable of stimulating T cells *per se* (Supplementary Figure S3).

LCs have traditionally been believed to have a role in the induction of CHS, but three research groups have reported three contradictory findings after applying haptens to transgenic mice deficient in LCs: a diminished reaction (Bennett *et al.*, 2005), an enhanced reaction (Kaplan *et al.*, 2005), and an unchanged response (Kissenpfennig *et al.*, 2005). Moreover, recent findings suggest that dDCs has a critical role in initiating CHS (Fukunaga *et al.*, 2008). In our study, dDCs augmented iNOS expression in response to hapten application more than LCs did. Our findings suggest that iNOS can suppress cutaneous DC migration and survival. Given that, in CHS, dDCs and LCs have positive and regulatory capacities, respectively, our findings on cutaneous DCs seem to be consistent with the observation that iNOS inhibitor induces an enhancement of CHS.

The findings of our study are clinically relevant in two respects. First, iNOS and NO exert immunosuppressive effects on cutaneous inflammation. In this context, the *in vivo* immunosuppressive effect of NO has also been shown in human studies (Kuchel *et al.*, 2003). Second, iNOS reduces cutaneous DC function and survival in the sensitization phase of CHS. The observation that NO directly reduces the number of LCs in the human epidermis supports our conclusion (Mowbray *et al.*, 2008).

MATERIALS AND METHODS

Animals and reagents

Female B6 mice were purchased from Japan SLC (Hamamatsu, Japan). All experiments were conducted on 8-week-old mice. The mice were maintained on a 12-hour light/dark cycle under a specific pathogen-free condition. All protocols were approved by the Institutional Animal Care and Use Committee of the University of Occupational and Environmental Health. L-NIL (a highly selective inhibitor of iNOS enzymatic activity) and LPS were obtained from Sigma-Aldrich (St Louis, MO). CCL21 was purchased from R&D Systems (Minneapolis, MN).

DNFB-induced CHS model

B6 mice were sensitized through the application of 25 μl of 0.5% (v/v) DNFB in 4:1 acetone/olive oil to their shaved abdomens on day 0. They were then challenged on both sides of each ear with 20 μl of 0.3% (v/v) DNFB. Ear thickness change was calculated as follows: (ear thickness 24 or 48 hours after challenge)−(ear thickness before challenge). iNOS was inhibited with L-NIL as described previously (Diefenbach *et al.*, 1998). Briefly, L-NIL was applied by intraperitoneal injection (2.5 mg in 0.5 ml PBS twice daily) for 6 consecutive days starting 1 day before sensitization. We chose his protocol because treatment with L-NIL at this concentration and frequency for 4-13 days is one of the most common methods of blocking *in vivo* activity of iNOS (Diefenbach *et al.*, 1998; Stallmeyer *et al.*, 1999).

EC preparation and culture

EC suspensions were prepared as described previously (Tokura *et al.*, 1994). Ears of naive mice were split along the plane of the cartilage, which was then removed together with the subcutaneous tissue. These specimens were incubated for 1 hour at 37 °C in a 0.2% solution of trypsin in PBS. After incubation, the epidermis was separated from the dermis and the separated epidermal sheets were rubbed to disperse the ECs in PBS supplemented with 10% fetal calf serum. The cells were filtered and washed twice in PBS. As a culture medium, RPMI-1640 (Sigma-Aldrich) was supplemented with 10% heat-inactivated fetal calf serum, 5×10^{-5} M 2-mercaptoethanol, 2 mM L-glutamine, 25 mM HEPES (4-(2-hydroxyethyl)-1-piperazineethanesulfonic acid), 1 mM nonessential amino acids, 1 mM sodium pyruvate, 100 U ml^{-1} penicillin, and 100 μg ml^{-1} streptomycin.

Preparation of dermal cell suspensions

Dermal cells were obtained from normal murine skin from which the epidermis had been removed. Samples were minced and incubated for 2 hours at 37 °C in RPMI-1640 medium (Invitrogen, Carlsbad, CA) supplemented with collagenase (2 mg ml^{-1}; Sigma-Aldrich), hyaluronidase (260 U ml^{-1}; Sigma-Aldrich), DNase (0.1 mg ml^{-1}; ICN, Costa Mesa, CA), and 10 mM HEPES (Sigma-Aldrich). The obtained cells were filtered through a 40-μm filter.

Flow cytometry

For flow cytometry, cells were plated at a density of 1×10^6 cells per well in 96-well U-bottomed plates (Falcon, BD Biosciences, San Jose, CA). Cells were then stained for 20 minutes on ice with mAbs in 25 μl of PBS containing 2% fetal calf serum, 1 mM EDTA, and 0.1% NaN_3, and washed twice with 200 μl of this buffer. Data were collected on a FACSCanto system (BD Biosciences) and analyzed with FlowJo software (TreeStar, San Carlos, CA). The mAbs used were as follows: FITC-conjugated anti-CD86 and Annexin V mAbs, PE-conjugated anti-CD80 and CD40 mAbs, PE-Cy5-conjugated anti-MHC class II mAb, APC-conjugated anti-CD11c mAb (all from BD Biosciences), and PE-Cy7-conjugated anti-CCR7 mAb (eBioscience, San Diego, CA). For detection of Langerin and iNOS, anti-Langerin Ab (eBioscience), PE-conjugated anti-iNOS Ab (Santa Cruz Biotechnology, Santa Cruz, CA), and PE-Cy5-conjugated streptavidin were

used after fixation and permeabilization of cells using a Cytofix/Cytoperm Kit (BD Biosciences).

Histology

At 48 hours after the challenge with hapten, the ears of B6 mice were excised and fixed in 10% formaldehyde. Sections of 5-μm thickness were prepared and stained with hematoxylin and eosin.

FITC-induced cutaneous DC migration

The shaved abdomens of the mice were painted with 200 μl of 2% FITC (Sigma-Aldrich) dissolved in a 1:1 (v/v) acetone/dibutyl phthalate (Sigma-Aldrich) mixture, and the iNOS inhibitor was applied through intraperitoneal injection (2.5 mg in 0.5 ml PBS) twice daily for 4 days. Cutaneous DCs migrating into the draining inguinal and axillary lymph nodes were then counted by means of flow cytometry (Kabashima *et al.*, 2007) using Flow-Count Fluorospheres (Beckman Coulter, Fullerton, CA). The principle of Flow-Count Fluorospheres is based on the precise mixing of microparticles whose concentration and volume are known. Before flow cytometric analysis, 10 μl of Flow-Count Fluorospheres were added to each specimen. The percentages of fluorospheres and migrating DCs within each node were then determined using the FACSCanto system (BD Biosciences). To find the number of migrating DCs, the ratio of DCs to fluorospheres was counted using the following formula, based on Reimann *et al.* (2000), with some modifications: number of migrating DCs = (percentage of migrating DCs/percentage of fluorospheres) × number of fluorospheres.

Chemotaxis assay

EC suspensions were incubated for 9 hours with or without the iNOS inhibitor, and then tested for transmigration across uncoated 5-μm transwell filters (Corning Costar, Corning, NY) to CCL21 or medium in the lower chamber for 3 hours. Migrating cells were enumerated by means of flow cytometry (Ngo *et al.*, 1998). The medium used in this assay was RPMI-1640 with 0.5% fatty acid-free bovine serum albumin (Calbiochem, San Diego, CA).

Apoptosis analysis

The EC suspensions from B6 mice were stained with PE-Cy5-conjugated anti-MHC class II mAb for 20 minutes on ice, then stained with FITC-conjugated Annexin V and propidium iodide (BD Pharmingen, Franklin Lakes, NJ), according to the manufacturer's protocol. The number of LCs was assessed by means of flow cytometry with anti-MHC class II and APC-conjugated anti-CD11c mAbs. Apoptosis in LCs was analyzed using a FACSCanto system with FlowJo software.

Statistical analysis

Data were analyzed using an unpaired two-tailed *t*-test. $P<0.05$ was considered to be significant.

CONFLICT OF INTEREST

The authors state no conflict of interest.

ACKNOWLEDGMENTS

This work was supported in part by a Grant-in-Aid for Scientific Research from the Ministry of Education, Culture, Sports, Science, and Technology of Japan, the Ministry of Health, Labor, and Welfare of Japan, and by a Grant from Shiseido Co. Ltd.

SUPPLEMENTARY MATERIAL

Supplementary material is linked to the online version of the paper at http://www.nature.com/jid

REFERENCES

Akiba H, Kehren J, Ducluzeau MT, Krasteva M, Horand F, Kaiserlian D *et al.* (2002) Skin inflammation during contact hypersensitivity is mediated by early recruitment of CD8+ T cytotoxic 1 cells inducing keratinocyte apoptosis. *J Immunol* 168:3079–87

Arany I, Brysk MM, Brysk H, Tyring SK (1996) Regulation of inducible nitric oxide synthase mRNA levels by differentiation and cytokines in human keratinocytes. *Biochem Biophys Res Commun* 220:618–22

Bennett CL, van Rijn E, Jung S, Inaba K, Steinman RM, Kapsenberg ML *et al.* (2005) Inducible ablation of mouse Langerhans cells diminishes but fails to abrogate contact hypersensitivity. *J Cell Biol* 169:569–76

Cals-Grierson MM, Ormerod AD (2004) Nitric oxide function in the skin. *Nitric Oxide* 10:179–93

Cruz MT, Neves BM, Goncalo M, Figueiredo A, Duarte CB, Lopes MC (2007) Effect of skin sensitizers on inducible nitric oxide synthase expression and nitric oxide production in skin dendritic cells: role of different immunosuppressive drugs. *Immunopharmacol Immunotoxicol* 29:225–41

Diefenbach A, Schindler H, Donhauser N, Lorenz E, Laskay T, MacMicking J *et al.* (1998) Type 1 interferon (IFNalpha/beta) and type 2 nitric oxide synthase regulate the innate immune response to a protozoan parasite. *Immunity* 8:77–87

Fukunaga A, Khaskhely NM, Sreevidya CS, Byrne SN, Ullrich SE (2008) Dermal dendritic cells, and not Langerhans cells, play an essential role in inducing an immune response. *J Immunol* 180:3057–64

Kabashima K, Shiraishi N, Sugita K, Mori T, Onoue A, Kobayashi M *et al.* (2007) CXCL12–CXCR4 engagement is required for migration of cutaneous dendritic cells. *Am J Pathol* 171:1249–57

Kaplan DH, Jenison MC, Saeland S, Shlomchik WD, Shlomchik MJ (2005) Epidermal Langerhans cell-deficient mice develop enhanced contact hypersensitivity. *Immunity* 23:611–20

Kissenpfennig A, Henri S, Dubois B, Laplace-Builhe C, Perrin P, Romani N *et al.* (2005) Dynamics and function of Langerhans cells *in vivo*: dermal dendritic cells colonize lymph node areas distinct from slower migrating Langerhans cells. *Immunity* 22:643–54

Kissenpfennig A, Malissen B (2006) Langerhans cells—revisiting the paradigm using genetically engineered mice. *Trends Immunol* 27:132–9

Kuchel JM, Barnetson RS, Halliday GM (2003) Nitric oxide appears to be a mediator of solar-simulated ultraviolet radiation-induced immunosuppression in humans. *J Invest Dermatol* 121:587–93

Lu L, Bonham CA, Chambers FG, Watkins SC, Hoffman RA, Simmons RL *et al.* (1996) Induction of nitric oxide synthase in mouse dendritic cells by IFN-gamma, endotoxin, and interaction with allogeneic T cells: nitric oxide production is associated with dendritic cell apoptosis. *J Immunol* 157:3577–86

Morita H, Hori M, Kitano Y (1996) Modulation of picryl chloride-induced contact hypersensitivity reaction in mice by nitric oxide. *J Invest Dermatol* 107:549–52

Mowbray M, Tan X, Wheatley PS, Rossi AG, Morris RE, Weller RB (2008) Topically applied nitric oxide induces T-lymphocyte infiltration in human skin, but minimal inflammation. *J Invest Dermatol* 128: 352–60

Musoh K, Nakamura N, Ueda Y, Inagaki N, Nagai H (1998) Possible role of nitric oxide in IgE-mediated allergic cutaneous reaction in mice. *Int Arch Allergy Immunol* 115:91–6

Nagao K, Ginhoux F, Leitner WW, Motegi SI, Bennett CL, Clausen BE *et al.* (2009) Murine epidermal Langerhans cells and langerin-expressing dermal dendritic cells are unrelated and exhibit distinct functions. *Proc Natl Acad Sci USA* 106:3312–7

Ngo VN, Tang HL, Cyster JG (1998) Epstein–Barr virus-induced molecule 1 ligand chemokine is expressed by dendritic cells in lymphoid tissues and strongly attracts naive T cells and activated B cells. *J Exp Med* 188:181–91

Ormerod AD, Dwyer CM, Reid A, Copeland P, Thompson WD (1997) Inducible nitric oxide synthase demonstrated in allergic and irritant contact dermatitis. *Acta Derm Venereol* 77:436–40

Qureshi AA, Hosoi J, Xu S, Takashima A, Granstein RD, Lerner EA (1996) Langerhans cells express inducible nitric oxide synthase and produce nitric oxide. *J Invest Dermatol* 107:815–21

Reimann KA, O'Gorman MR, Spritzler J, Wilkening CL, Sabath DE, Helm K *et al.* (2000) Multisite comparison of CD4 and CD8 T-lymphocyte counting by single- versus multiple-platform methodologies: evaluation of Beckman Coulter flow-count fluorospheres and the tetraONE system. The NIAID DAIDS New Technologies Evaluation Group. *Clin Diagn Lab Immunol* 7:344–51

Rocha IM, Guillo LA (2001) Lipopolysaccharide and cytokines induce nitric oxide synthase and produce nitric oxide in cultured normal human melanocytes. *Arch Dermatol Res* 293:245–8

Ross R, Gillitzer C, Kleinz R, Schwing J, Kleinert H, Forstermann U *et al.* (1998) Involvement of NO in contact hypersensitivity. *Int Immunol* 10:61–9

Ross R, Reske-Kunz AB (2001) The role of NO in contact hypersensitivity. *Int Immunopharmacol* 1:1469–78

Saeki H, Moore AM, Brown MJ, Hwang ST (1999) Cutting edge: secondary lymphoid-tissue chemokine (SLC) and CC chemokine receptor 7 (CCR7) participate in the emigration pathway of mature dendritic cells from the skin to regional lymph nodes. *J Immunol* 162:2472–5

Sanchez-Sanchez N, Riol-Blanco L, Rodriguez-Fernandez JL (2006) The multiple personalities of the chemokine receptor CCR7 in dendritic cells. *J Immunol* 176:5153–9

Schuler G, Steinman RM (1985) Murine epidermal Langerhans cells mature into potent immunostimulatory dendritic cells *in vitro*. *J Exp Med* 161:526–46

Stallmeyer B, Kampfer H, Kolb N, Pfeilschifter J, Frank S (1999) The function of nitric oxide in wound repair: inhibition of inducible nitric oxide-synthase severely impairs wound reepithelialization. *J Invest Dermatol* 113:1090–8

Sugita K, Kabashima K, Atarashi K, Shimauchi T, Kobayashi M, Tokura Y (2007) Innate immunity mediated by epidermal keratinocytes promotes acquired immunity involving Langerhans cells and T cells in the skin. *Clin Exp Immunol* 147:176–83

Tokura Y, Yagi J, O'Malley M, Lewis JM, Takigawa M, Edelson RL *et al.* (1994) Superantigenic staphylococcal exotoxins induce T-cell proliferation in the presence of Langerhans cells or class II-bearing keratinocytes and stimulate keratinocytes to produce T-cell-activating cytokines. *J Invest Dermatol* 102:31–8

Wang R, Ghahary A, Shen YJ, Scott PG, Tredget EE (1996) Human dermal fibroblasts produce nitric oxide and express both constitutive and inducible nitric oxide synthase isoforms. *J Invest Dermatol* 106:419–27

Yamaoka J, Kume T, Akaike A, Miyachi Y (2000) Suppressive effect of zinc ion on iNOS expression induced by interferon-gamma or tumor necrosis factor-alpha in murine keratinocytes. *J Dermatol Sci* 23:27–35